

Cream of the Crop: Harvesting Rich, Scalable and Transferable Multi-Modal Data for Instruction Fine-Tuning

Mengyao Lyu^{1,2} Yan Li³ Huasong Zhong³ Wenhao Yang³ Hui Chen^{1,2} Jungong Han^{1,2}
Guiguang Ding^{1,2} Zhenheng Yang³

Abstract

The hypothesis that pretrained large language models (LLMs) necessitate only minimal supervision during the fine-tuning (SFT) stage (Zhou et al., 2024) has been substantiated by recent advancements in data curation and selection research. However, their stability and generalizability are compromised due to the vulnerability to experimental setups and validation protocols, falling short of surpassing random sampling (Diddee & Ippolito, 2024; Xia et al., 2024b). Built upon LLMs, multi-modal LLMs (MLLMs), combined with the sheer token volume and heightened heterogeneity of data sources, amplify both the significance and complexity of data selection.

To harvest multi-modal instructional data in a robust and efficient manner, we re-define the granularity of the quality metric by decomposing it into 14 vision-language-related capabilities, and introduce multi-modal rich scorers to evaluate the capabilities of each data candidate. To promote diversity, in light of the inherent objective of the alignment stage, we take interaction style as diversity indicator and use a multi-modal rich styler to identify data instruction patterns. In doing so, our **multi-modal rich scorers and styler** (mmSSR) guarantee that high-scoring information is conveyed to users in diversified forms. Free from embedding-based clustering or greedy sampling, mmSSR efficiently scales to millions of data with varying budget constraints, supports customization for general or specific capability acquisition, and facilitates training-free generalization to new domains for curation. Across 10+ experimental settings, validated by 14 multi-modal benchmarks, we demonstrate consistent improvements over random sampling, baseline strategies and state-of-the-art selection methods, achieving 99.1% of full performance with only 30% of the 2.6M data³.

¹Tsinghua University ²BNRist ³Bytedance (work as an intern).
Correspondence to: Guiguang Ding <dinggg@tsinghua.edu.cn>.

³ <https://lyumengyao.github.io/projects/mmssr>

1. Introduction

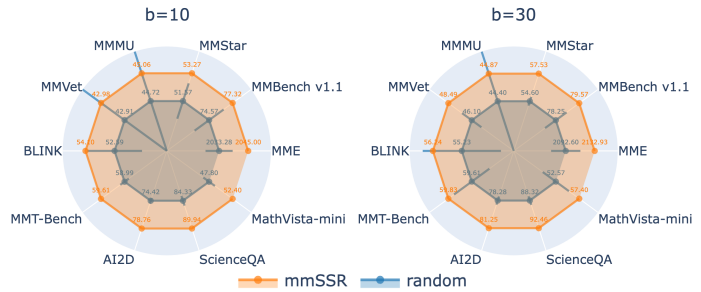


Figure 1. Our proposed mmSSR against the random sampling baseline (3 trials) across both general and specialized multi-modal benchmarks under the 10% (L) and 30% (R) data budgets.

The quality of data matters in the scaling of large models (Li et al., 2024b; Wettig et al., 2024; Liu et al., 2024b; Lu et al., 2024; Luo et al., 2024; Li et al., 2024a). It is particularly important during their supervised fine-tuning (SFT) stage, where pre-trained models are expected to efficiently and accurately follow user instructions for general purposes or specialized deployment. To achieve this, earlier approaches for large language models (LLMs) filter large-scale SFT datasets with millions of samples towards redundancy reduction (Lee et al., 2022; Elazar et al., 2024), quality control and safety regulation (Joulin, 2016; Penedo et al., 2023; Dubey et al., 2024; Team et al., 2024; Chung et al., 2024). Recently, LIMA introduces the superficial alignment hypothesis (SAH) (Zhou et al., 2024), which utilizes only 1,000 carefully curated samples to illustrate that most LLM knowledge has been acquired during pre-training, requiring only minimal data for instruction fine-tuning, and the effectiveness of these few samples hinges on their quality and diversity. This shift has encouraged subsequent research on automated sample selection, which aims to identify and extract valuable data on these key attributes (Lu et al., 2024; Xia et al., 2024a; Liu et al., 2025), thereby reducing time and computational cost while enhancing interpretability of the target models. However, although the SAH remains valid under the verification of hand-crafted data, recent surveys (Diddee & Ippolito, 2024; Xia et al., 2024b) reveal that automated sample selection methods are susceptible to

experimental conditions, including variations in available budgets, different data sources and diverse evaluation benchmarks, which hinders them to get consensus on benchmarks or consistently outperform uniform sampling in generalization. And their reliance on data embedding to promote subset diversity could end up making the entire process inefficient and unable to scale up (Zhou et al., 2023; Liu et al., 2024b; Pang et al., 2024; Li et al., 2024c).

Building on the challenges in data selection for LLMs, we first shift our focus to multi-modal LLMs (MLLMs), where the increased variety of data modalities, combined with the sheer token volume and heterogeneity of data sources, elevate the significance of data selection as a critical yet underexplored aspect of model performance. First, unlike their text-only counterparts, the selection algorithm must be adept at identifying samples that not only exhibit high quality and diversity within each modality but capture the underlying correlations between them. On the other hand, MLLMs pose new challenges in achieving generalization across various settings and tasks due to the pronounced noise and variability inherent in the multi-modal data curation process (Chen et al., 2024a; Li et al., 2024a; Liu et al., 2024a). Furthermore, the sensitivity of sample selection methods of LLMs prevents their direct adaptation to MLLMs, and the vision-language (VL) alignment metrics adopted by VL models (VLMs) (Maini et al., 2024; Gadre et al., 2023) is not aligned with the motivation of instruction alignment, showing suboptimal performance (See our results in Sec. 4.2) These observations necessitate innovative approaches for multi-modal data selection to cut computational consumption and improve data understanding (Wang et al., 2024a).

In response to the challenges of multi-modal data selection in valuation coverage, data scaling and transferability, we propose to decompose the complexity of data into rich capabilities that are human-interpretable and model-attributable (such as spatial understanding, logical deduction), which breaks down abstract concepts into multiple concrete metrics that can be systematically evaluated. In this paper, we exemplify 14 criteria that serve as the foundational pillars for the development of vision perception and reasoning capabilities, and train corresponding scorers to provide assessments on each candidate. In comparison to vague formulation such as *quality* or *complexity* (Liu et al., 2024b; Pang et al., 2024), our rich scores re-define the granularity of data valuation, facilitating improved understanding, easy customization and better transferability. Different from potentially task-specific metric or model-dependent predictions, the concrete criteria we propose carry clear and general semantics that can be easily exposed from the pre-trained model, so that our instructed scorers will not overfit to the training data if the existing data pool is limited, yielding robust transferability across tasks and domains. Equipped with rich scores

of multi-modal instances, ensuring data diversity becomes a critical next step, especially for large-scale multi-modal heterogeneous mixtures. In light of the nature of the instruction tuning stage, where the model learns to interact with users in different styles (Zhou et al., 2024), we take the superficial instruction styles as a straightforward indicator of diversity, and introduce a multi-modal rich styler to cluster instances based on their interaction patterns. Free from in-domain feature representation learning (Lee et al., 2024), distance-based greedy filtering and cluster-based sampling (Liu et al., 2024b; Lee et al., 2024), the instance-level style clustering significantly reduces computational complexity and becomes scalable. In our experiments on the LLaVA-OneVision (LLaVA-OV) (Li et al., 2024a), the state-of-the-art (SOTA) open MLLM series with a well-curated dataset, we demonstrate the significance of our **multi-modal Rich Scorer and Styler (mmSSR)** across 6 varying budget settings and 2 different model sizes, comprehensively validated with 14 benchmarks. We further evaluate the practicality of mmSSR towards domain generalization and its scalability in data quantity and capability. To the best of our knowledge, this is the first selection method aimed at an open-source, SOTA data pool with *millions of multi-modal SFT entries*, facilitating efficient adaptation, flexible customization, and offering new perspectives for model understanding. The main contributions are summarized as follows:

- We present a novel data selection pipeline for multi-modal instruction data, which decomposes the complexity of the problem into rich capability scores and styles and trains mmSSR for data valuation.
- mmSSR demonstrates superiority in performance, scalability and transferability, as comprehensively validated across 10 settings with 14 general and specialized benchmarks.
- The pre-tuned mmSSR, along with our instruction data and selected subsets of LLaVA-OV, can be readily utilized by the community for domain generalization, new capability acquisition, and result replication.

2. Related Work

Recent advances have explored various strategies to improve data efficiency. While research on MLLMs remains limited, our work draws inspiration from existing studies for LLMs, vision-language models (VLMs), and active learning. These efforts can be broadly categorized hand-crafted heuristics, model-based indicators, and LLM-based scoring. They can be inter-changeably or complementarily applied across different training stages.

Hand-Crafted Heuristics rely on expert knowledge on the specific task to establish quality metrics for data filtering

or selection. From high-level features such as relevance, clarity, diversity and safety to lower-level indicators like vocabulary, N-gram and sentence length (Team et al., 2023; Touvron et al., 2023; Dubey et al., 2024; Qin et al., 2024; Penedo et al., 2023). While these heuristics are interpretable and straightforward to implement, they are labor-intensive and often prone to human bias, and lack adaptability to iterate target models and to multi-modal data challenges.

Model-Based Indicators often leverage the internal mechanisms or outputs of target models to assess data. Across machine learning algorithms and recent large models, a common paradigm leverages the gradients, predictive distributions, and embeddings of the target model to assess uncertainty, entropy, learnability, similarity and transferability (Evans et al., 2024; Liu et al., 2024c; Lyu et al., 2023; 2025; Sener & Savarese, 2018; Liu et al., 2024b; 2025; Settles, 2009). These approaches could offer promising in-domain performance when the computational cost of target models are affordable. However, judgments made by models may also struggle with interpretability and transferability (Diddee & Ippolito, 2024; Munjal et al., 2020). Introducing proxy models into the data selection pipeline mitigates dependency on the task model. One widely adopted strategy is to train bigram or unigram classifiers (Joulin, 2016; Brown et al., 2020; Gao et al., 2025; Li et al., 2024b) with a vast amount of text data collection, which poses challenges in generalizing such methods to MLLMs. Recently, COINCIDE (Lee et al., 2024) introduces a tiny 2B trained on the 665K target data pool to extract data embedding for the core-set (Sener & Savarese, 2018) selection. However, the use of the entire target dataset diminishes the significance of data selection. And high-dimensional embedding-based clustering and greedy sampling also pose scalability challenges. Despite the rarity of exploration for MLLMs, VLM research has proposed several multi-modal quality metrics that considers alignment as the objective (Maini et al., 2024; Gadre et al., 2023; Goyal et al., 2024). However, these scores do not necessarily correlate with optimal MLLM performance and may inadvertently select repetitive or redundant data points. Thus, balancing in-domain performance an cross-domain generalization still poses a great challenge for data selection studies. Built upon the pretrained target model, our obtained mmSSR can effectively follow the instruction of scoring and styling while the transferability of our fine-grained capabilities is well retained, as validated in Sec. 4.3.

LLM-Based Scoring employs a teacher model, such as proprietary ChatGPT (Brown et al., 2020; Achiam et al., 2023), as a cost-effective alternative to human annotation for scoring or ranking candidate instances. QuRating (Wettig et al., 2024) formulates four qualities regarding the quality of pretraining corpora, yet these qualities are investigated in isolation rather than being considered as composable.

Deita (Liu et al., 2024b) defines the valuation of instructional data in terms of *quality* and *complexity*, and prompts ChatGPT (Achiam et al., 2023) to generate data that evolve in the two dimensions for training scorers. DS² directly prompts for scores in *rarity*, *complexity*, and *informativeness* for all candidate data points. We find that those high-level quality dimensions identified for LLM data are insufficient to capture the variability and inherent in multi-modal data concerning complex VL benchmarks. Furthermore, sample-level or pairwise scoring fails to account for global diversity, which is particularly crucial for SFT. And their chosen embedding-based thresholding are challenging to scale up. Our mmSSR also built upon GPT-4o (Achiam et al., 2023) judgments. However, we emphasize that the decomposition of model capabilities to the concrete level enriches the multi-modal data scoring while the style identification significantly simplify the selection procedure, enabling it to be customizable, effective, transferable, and scalable to the SOTA multi-modal open dataset.

3. Method

3.1. Problem Formulation and Overview

In this paper, we study the problem of data selection for MLLMs towards instruction alignment. Given a large-scale data pool $D = \{X_1, X_2, \dots, X_N\}$, where each instance x_i consists of multiple modalities, our task is to find a subset D_{sel} of size b that optimize the instruction following ability of the target model. Here we consider image and question-answer pairs, i.e., $X_i = (I_i, Q_i, A_i)$. The data budget b is constrained by the computational budget of the SFT stage.

Our pipeline is built upon four key resources: a pretrained MLLM model (\mathcal{M}_θ), a curated list of VL capabilities (C), a list of interaction styles (S) that support the instruction tuning of MLLMs, and a budget to assess a small amount of randomly sampled data X' . As shown in Fig. 2, our strategy includes four steps: (i) We employ GPT-4o to generate judgments on X' , which encompasses the range of visual concepts in (C) and assigns multiple style from the label space S ; (ii) We finetune \mathcal{M}_θ with the subset and their corresponding scores and styles, yielding a series of Scr_i and Sty_i ; (iii) We infer on the whole data pool with respect to the rich capabilities and styles and perform style-aware top-score selection, yielding the selected subset \hat{X} where $|\hat{X}| = b$; (iv) the pretrained model is efficiently finetuned with the subset. Once the mmSSR is obtained, within the domain of D , the composition of Scr_i can be customized towards general instruction tuning purposes or adapted for specialized requirements; one can also directly transfer mmSSR to new domain for data selection.

Next, we discuss the major contributions of our pipeline: formulating data quality valuation into *rich* and *transferable*

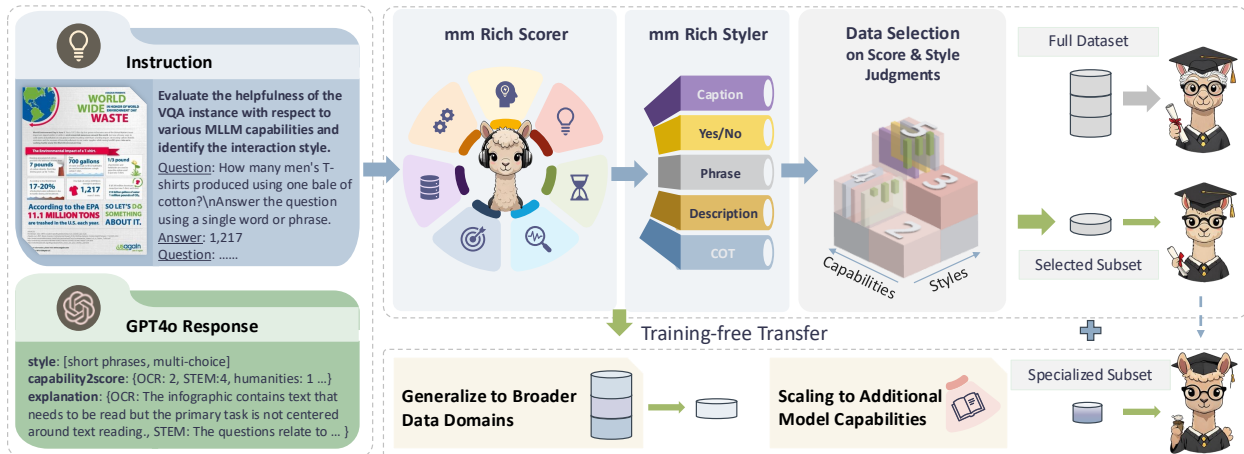


Figure 2. Pipeline of the proposed multi-modal data selection method. We decompose the VL capabilities required by MLLMs and refer to GPT-4o’s judgments of the rich capabilities on a scale from 0 to 5, while meantime prompting the identification of the user-model interaction style. The small amount of derived sample-scores-styles triplets is employed to instruct the pretrained task model for **multi-modal rich scorers** and **styler**, i.e., our **mmSSR**. It facilitates the analysis and sampling of candidate data points at the scale of millions, ensuring a subset that is both high-quality and diverse, while maintaining minimal time and resource expenditure. The fine-grained **mmSSR** can also directly generalize to other data domains, and support efficient scaling in data quantity and capabilities.

capability criteria via scorers to build up MLLMs (Sec. 3.2), promoting data diversity via an instruction styler for efficient and *scalable* SFT (Sec. 3.3), and implementing style-aware, score-prioritized data selection (Sec. 3.4).

3.2. Multi-modal Rich Scorers

In the context of data valuation, especially for the instructional data, integrating advanced proprietary model, e.g., ChatGPT (Brown et al., 2020; Achiam et al., 2023), as a teacher has proven to be an effective automatic scoring approach given its high alignment with human preferences regarding conversation quality (Liu et al., 2024b; Pang et al., 2024; Wettig et al., 2024; Wang et al., 2024c; Yuan et al., 2024). A crucial aspect of this approach lies in the formulation of the scoring task, namely, formulating clear metrics and guidelines to instruct the model to query scores that are aligned with the optimization of MLLMs. We expect each instance-level score to exhibit clarity in multi-modal criteria, reliability in value and consistency across the entire data pool. However, we find that high-level, abstract keywords, such as quality, complexity (Pang et al., 2024; Liu et al., 2024b), accuracy and difficulty (Xu et al., 2023) adopted by previous selection methods for LLMs, fall short in capturing the complexity of our data with a greater variety of data modalities, a larger volume of data tokens, and a more heterogeneous pool of sources.

To overcome these challenges, we first enhance *clarity* by redefining the granularity of the scoring task, decomposing it into 14 specific capabilities: *object spatial understand-*

ing, attribute identification, logical deduction, scene understanding, fine-grained recognition, language generation, in-context learning, comparative analysis, activity recognition, causal reasoning, humanities, stem knowledge, data understanding and optical character recognition (OCR). These capabilities are both human-interpretable and model-attributable, covering rich visual-textual information. Meantime, we provide brief explanations of these criteria (detailed in Appendix A.2) to further simplify the scoring task and instruct it to align with human understanding. To improve the *reliability* of the score value, we further request GPT-4o to explain the rationale behind why a score is not higher or lower, in order to improve its answer in a self-reflection manner. As for cross-instance score *consistency*, to avoid overly lengthy prompt for VL inputs and changes in the finetuning paradigm, instead of prompting pairwise, we specifically clarify the level of helpfulness for each value scale, which improves applicability across all capabilities and instances. Our prompt for scoring can be found in Appendix A.2.

To ensure cost-effectiveness, scalability and wide applicability, we randomly sample a small portion of data X' (15% in our main experiment) from the target data pool to query GPT-4o \mathcal{G} for scores across all capabilities: $\mathcal{S}cr(X_i) = \{\mathcal{G}(I_i, Q_i, A_i; c_j)\}$, where c_j is the j -th capability. The paired data-score instances $(X_i, \mathcal{S}cr(X_i))$ are then used to instruct a multi-modal model to predict rich scores for the 14 criteria. Thus, we can optimize the selection of comprehensive and general-purpose multi-modal datasets or construct specialized data mixtures as needed according to the judgments of our multi-modal rich scorers. In addition

to the advantages of being rich, scalable, and customizable, our fine-grained decomposition of the scoring task ensures its transferability. As the capabilities we exemplify clear and general semantics, during the scoring SFT, the understanding of capability semantics of the pre-trained model is exposed through the interactive scoring task, rather than merely fitting a limited amount of training data. When the capability semantics themselves are clear and general, the obtained fine-grained scorers exhibit strong transferability.

3.3. Multi-modal Rich Styler

Data selection research for LLMs has revealed that data diversity is crucial, particularly during the supervised finetuning (SFT) stage (Zhou et al., 2024; Diddee & Ippolito, 2024; Xia et al., 2024b; Liu et al., 2024b; Pang et al., 2024; Li et al., 2024c). This challenge is further exacerbated by the heterogeneity of multi-modal data. For instance, the single-image training stage of LLaVA-OV (Li et al., 2024a) draws images from more than ninety different sources. To ensure selection diversity, existing studies derive the D -dim deep feature as data representations, upon which the similarity computations and k-means greedy sampling are conducted within a complexity of $\mathcal{O}(NkD)$ (Liu et al., 2024b; Lee et al., 2024). Despite being straight-forward, the computationally burdensome strategy struggles to handle data of multi-modality in the magnitude of millions.

In light of the SAH (Zhou et al., 2024) that the main focus of SFT is to learn the interaction styles with users rather than acquiring new knowledge, we argue that the *superficial* styles can be a cheap and efficient proxy to capture interaction diversity. We curate a list of 9 styles observed in the current data pool (detailed in Tab. 3). Similar to the data curation for scorer training, we query GPT-4o on the presence of each style s_j : $Sty(X_i) = \{\mathcal{G}(I_i, Q_i, A_i; s_j)\}$. Then the data-style pairs $(X_i, Sty(X_i))$ are used to instruct a model so as to infer rich styles on the entire data pool.

Compared to a large quantity of heuristic cluster centers ($k > 10,000$), utilizing concise and semantically rich data proxy (9 for mmSSR) enables us to efficiently bucket the data in $\mathcal{O}(N)$ inference time, thereby avoiding the quadratic similarity calculations based on embeddings and the k-center hyperparameter tuning. The shift in perspective from traditional distribution-based sampling to style-based clustering not only ensures scalability as data continues to grow, but also directly facilitates the training objectives during the instruction tuning phase. Conversely, the effectiveness of the styler, as validated in our experiments, also demonstrates the applicability of SAH within the MLLM paradigm.

3.4. mmSSR for Data Selection

Given any set of capabilities of interest \hat{C} , the corresponding mmSSR are readily prepared to infer on the candidate data

pool, obtaining a score vector $\hat{S}^{cr_i} = \{r_{ic}\}$ where the score $r_{ic} \in [0, 1, \dots, 5]$, and a style vector $\hat{S}^{ty_i} = \{g_{is}\}$ where the style membership is given by $g_{is} \in [0, 1]$ for each instance X_i in D . To achieve capability balancing and style diversity, we traverse the dataset in a Round-Robin fashion. Specifically, we define $|\hat{C}| \times |S|$ groups, and group $G_{cs} = \{i | r_{ic} > 0, g_{is} = 1\}$ is the set of indices of data points that belong to the group cs . Given a budget b , we iterate over each group for the highest-scored $\lfloor \frac{b}{|\hat{C}| \times |S|} \rfloor$ samples without replacement until the budget runs out:

$$D_{sel} = \bigcup^{|\hat{C}| \times |S|} d_{cs} \quad \text{where } |d_{cs}| = \left\lfloor \frac{b}{|\hat{C}| \times |S|} \right\rfloor + \delta_{cs}, \quad (1)$$

and δ_{cs} accounts for the remainder to ensure $\sum^{|\hat{C}| \times |S|} |d_{cs}| = b$. To summarize, our mmSSR facilitates style-aware, score-prioritized sampling for multi-modal instructional data with efficiency and data scalability. Their formulation also guarantees transferability, customization and scalability in capabilities. We verify these features in the next experiment section.

4. Experiments

4.1. Experimental Setup

Data pool. We base our main experiments on the single-image SFT stage of LLaVA-OV (LLaVA-OVSI) (Li et al., 2024a), the current open-source, open-data SOTA MLLM series. Within its 3.2 million high-quality instances¹, 2.6 million multi-modal data are openly available, which we consider as the full dataset and perform sample selection on it. This well-curated dataset covers over 90 sources, encompassing natural images, math and reasoning questions, documents, charts, screenshots, and general OCR.

In our transfer experiments (Sec. 4.3), we use the earlier ShareGPT4V (Chen et al., 2024a) as the source data pool, which contains 624K image-question-answer pairs².

Training setup. For simplicity, we take the stage-1.5-7B checkpoint³ provided by LLaVA-OneVision as the pre-trained model for both mmSSR finetuning and single-image task model instruction tuning. To reduce the cost of comparative experiments, we decrease the maximum token length to 12k, ensuring that all training can be completed on 64 Nvidia H100 GPUs with a batch size of 128. Apart from this, all experimental settings strictly follow the training setup adopted by the official LLaVA-OneVision implementation.

¹<https://huggingface.co/datasets/lmms-lab/LLaVA-OneVision-Data>

²<https://huggingface.co/datasets/Lin-Chen/ShareGPT4V>

³<https://huggingface.co/lmms-lab/llava-onevision-qwen2-72b-mid-stage-a4>

Table 1. Performance comparison on multi-modal benchmarks across varying budgets of 5, 10 and 30 of LLaVA-OVSI. We highlight the best result in **boldface** and underline the result if it beats the random baseline. The column >Rand presents the number of benchmarks where the method exceeds random sampling, and /FULL compares the performance of sampled data with that of the FULL dataset.

	MMBench _{en-v1.1}	MMStar	MMMU	MMVet	BLINK	MMT-Bench	MME	AI2D	ScienceQA	MathVista _{mini}	>Rand	/FULL
Budget: 5%												
Random	73.74	47.98	43.70	42.34	50.61	58.87	2004.50	73.07	81.52	45.47	-	89.29
PPL-mid	67.34	45.27	38.98	30.18	45.27	54.33	1887.71	66.74	74.76	31.40	0/10	78.31
PPL-si	71.98	44.67	38.48	35.14	54.10	57.98	1856.79	67.84	78.24	36.50	1/10	83.10
Deita	72.91	47.47	41.28	40.23	<u>52.59</u>	56.57	1956.50	70.76	79.57	36.10	1/10	85.79
CLIP	<u>74.23</u>	47.27	40.08	35.73	<u>52.96</u>	56.73	1902.65	<u>73.61</u>	78.63	39.80	3/10	85.41
E5-V	70.90	43.00	38.78	38.44	49.94	54.65	1810.47	66.58	77.54	37.40	0/10	81.87
COINCIDE	72.76	<u>48.33</u>	43.17	45.60	49.43	57.50	1852.66	<u>73.15</u>	79.62	45.40	3/10	88.44
mmSSR	<u>77.79</u>	<u>53.33</u>	43.27	<u>43.53</u>	<u>51.83</u>	59.16	1938.68	77.66	88.45	52.00	8/10	93.20
Budget: 10%												
Random	74.57	51.57	44.72	42.91	52.59	58.99	2033.28	74.42	84.33	47.80	0/10	91.70
PPL-mid	63.54	46.87	39.08	36.93	45.90	54.30	1831.03	67.23	73.87	39.50	0/10	80.72
PPL-si	<u>74.69</u>	49.80	41.28	40.60	<u>53.09</u>	57.95	1841.11	<u>75.16</u>	80.71	40.40	3/10	87.63
Deita	<u>75.39</u>	48.80	43.77	42.25	54.48	57.40	1996.34	71.60	78.33	40.80	2/10	88.72
CLIP	<u>75.23</u>	49.87	40.38	37.16	<u>53.59</u>	<u>59.35</u>	1921.04	<u>76.62</u>	80.07	41.00	4/10	87.69
E5-V	70.51	45.13	38.78	39.59	50.57	55.10	1787.94	68.94	77.54	37.20	0/10	82.76
COINCIDE	<u>75.23</u>	49.73	<u>44.77</u>	42.52	50.69	58.71	2027.58	<u>74.77</u>	82.05	47.00	3/10	90.66
mmSSR	<u>77.32</u>	<u>53.27</u>	45.06	42.98	54.10	59.61	2045.00	78.76	89.94	52.40	10/10	94.75
Budget: 30%												
Random	78.25	54.60	44.40	46.10	55.23	59.61	2092.60	78.28	88.32	52.57	-	95.82
PPL-mid	73.99	<u>54.93</u>	43.97	41.01	53.09	58.78	2036.54	77.20	87.01	<u>56.40</u>	2/10	93.77
PPL-si	72.52	48.33	42.57	43.62	51.83	55.07	1976.46	76.55	78.48	42.20	0/10	88.22
Deita	76.93	54.13	43.67	44.04	55.11	<u>59.66</u>	2042.63	<u>79.50</u>	83.54	50.30	2/10	94.05
CLIP	74.30	53.80	43.07	45.87	51.95	59.16	2039.14	<u>80.02</u>	83.99	48.80	1/10	93.07
E5-V	74.30	46.07	43.27	<u>47.80</u>	50.32	57.85	1955.13	74.45	81.61	43.70	1/10	89.52
COINCIDE	78.02	<u>55.47</u>	45.66	<u>46.24</u>	52.84	<u>59.80</u>	2047.37	<u>79.73</u>	84.33	<u>55.10</u>	6/10	95.82
mmSSR	<u>79.57</u>	<u>57.53</u>	44.87	48.49	56.24	59.83	2132.93	81.25	92.46	57.40	10/10	99.11
FULL												
LLaVA-OVSI	80.57	59.40	45.16	47.16	56.87	60.73	2117.56	81.87	92.76	59.60	-	100

In our transfer experiments (Sec. 4.3), we use the architecture of LLaVA-1.5-7B (Liu et al., 2024a) as the backbone model to instruct mmSSR. Likewise, the finetuning procedure of scorers and styler strictly follows the original implementation, all conducted on 8 Nvidia A100.

Our setting. Unless otherwise specified, we consider all capabilities, except for OCR, in our sampling experiments. We withhold the OCR capability to demonstrate the scalability of mmSSR on different capabilities, as presented in Sec. 4.4. In our experiments, we additionally make use of the 91 sources of LLaVA-OVSI data as subdomains and subdivide the grouped data, ensuring diversity among high-value samples across both language and visual modalities.

Baselines. We compare mmSSR with 8 methods across 6 different categories: a) *random sampling*: the strong diversity-prioritized baseline, evaluated based on the average results from three trials of different random splits; b) *perplexity*, including its two variants before (PPL-mid) and after (PPL-si) the single-image SFT on the entire data

pool; c) *Deita* (Liu et al., 2024b)⁴, the score and embedding-based SOTA method for LLMs; d) *CLIP similarity* (Radford et al., 2021) (ViT-L) that evaluates the image-text alignment; e) *E5-V similarity* (Jiang et al., 2024), the SOTA MLLM-based universal embedding model built on LLaMA-3-8B (Dubey et al., 2024) that supports encoding longer textual sequences; and f) COINCIDE (Lee et al., 2024), the SOTA clustering-based selection strategy for MLLMs. To demonstrate the necessity of training proxy models, we directly prompt Qwen2-VL-7B (Wang et al., 2024b), the SOTA open-source MLLM, and the pre-tuned LLaVA-OVSI checkpoint for scores and styles with the same instruction.

Evaluation benchmarks. Under the VLMEvalKit (Duan et al., 2024) framework, we comprehensively evaluate our method on 14 multi-modal benchmarks, including MME (Fu et al., 2024a), MMBench_{en-v1.1} (Liu et al., 2023a), MMStar (Chen et al., 2024b), MMMU (Yue et al., 2024),

⁴As Deita controls sample diversity through embedding similarity, the $O(N^2)$ complexity and the cost associated with threshold tuning is prohibitively expensive for scaling to our target data pool of 2.6 million instances. Therefore, we employ a variant that performs top-k sampling with its quality and complexity scores.

Table 2. Ablation study of mmSSR. mmSSR(ich): original mmSSR; mmSSP(oor): query GPT-4o to score on abstract criterion and give explanation; mmSSR + X: use our rich prompt to direct query scores and styles from open model X. We highlight the best result in **boldface** and underline the result if it beats the random baseline. The column >Rand presents the number of benchmarks where the method exceeds random sampling, and /FULL compares the performance of sampled data with that of the FULL dataset.

	MMBench _{en-v1.1}	MMStar	MMMU	MMVet	BLINK	MMT-Bench	MME	AI2D	ScienceQA	MathVista _{MINI}	>Rand	/FULL
Budget: 5%												
Random	73.74	47.98	43.70	42.34	50.61	58.87	2004.50	73.07	81.52	45.47	-	89.29
mmSSP(oor)	<u>75.85</u>	<u>51.27</u>	42.97	44.27	<u>51.95</u>	58.14	1940.27	<u>73.61</u>	81.46	45.00	5/10	<u>90.14</u>
mmSSR + LLaVA-OVSI	<u>77.40</u>	<u>50.60</u>	<u>44.77</u>	41.10	54.35	58.62	1952.97	<u>75.81</u>	<u>87.75</u>	40.40	6/10	<u>90.68</u>
mmSSR + Qwen2-VL	<u>75.08</u>	<u>51.00</u>	45.16	<u>42.57</u>	<u>52.71</u>	57.37	1955.78	<u>74.74</u>	<u>84.88</u>	<u>48.90</u>	8/10	<u>91.37</u>
mmSSR(ich)	77.79	53.33	43.27	<u>43.53</u>	<u>51.83</u>	59.16	1938.68	77.66	88.45	52.00	8/10	93.20
Budget: 10%												
Random	74.57	51.57	44.72	42.91	52.59	58.99	2033.28	74.42	84.33	47.80	-	91.70
mmSSP(oor)	<u>77.24</u>	50.40	44.27	42.52	<u>53.47</u>	<u>59.48</u>	2084.39	<u>76.07</u>	81.36	46.10	5/10	<u>91.73</u>
mmSSR + LLaVA-OVSI	77.79	54.40	44.67	42.02	<u>54.98</u>	58.23	2013.74	78.85	<u>89.59</u>	42.00	5/10	<u>92.72</u>
mmSSR + Qwen2-VL	<u>76.24</u>	<u>53.33</u>	<u>44.87</u>	45.60	55.11	<u>59.16</u>	2012.94	<u>76.75</u>	<u>87.11</u>	52.70	9/10	<u>94.59</u>
mmSSR(ich)	<u>77.32</u>	<u>53.27</u>	45.06	42.98	<u>54.10</u>	59.61	2045.00	<u>78.76</u>	89.94	<u>52.40</u>	10/10	94.75
Budget: 30%												
Random	78.25	54.60	44.40	46.10	55.23	59.61	2092.60	78.28	88.32	52.57	-	95.82
mmSSP(oor)	77.86	53.13	45.76	<u>48.03</u>	54.85	58.78	2050.69	<u>78.92</u>	86.91	<u>55.80</u>	4/10	<u>96.31</u>
mmSSR + LLaVA-OVSI	77.55	54.53	43.37	44.72	55.23	58.59	1980.48	<u>81.02</u>	<u>91.87</u>	49.60	2/10	94.73
mmSSR + Qwen2-VL	78.02	<u>57.13</u>	43.07	<u>47.39</u>	<u>55.49</u>	60.89	<u>2096.60</u>	81.64	<u>90.28</u>	57.40	8/10	<u>97.91</u>
mmSSR(ich)	79.57	57.53	<u>44.87</u>	48.49	56.24	<u>59.83</u>	2132.93	<u>81.25</u>	92.46	57.40	10/10	99.11
FULL												
LLaVA-OVSI	80.57	59.40	45.16	47.16	56.87	60.73	2117.56	81.87	92.76	59.60	-	100

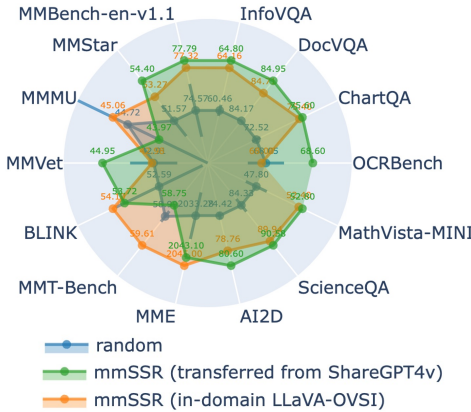


Figure 3. Transferability of mmSSR models: trained on ShareGPT4v data, directly inferences on large-scale LLaVA-OVSI pool.

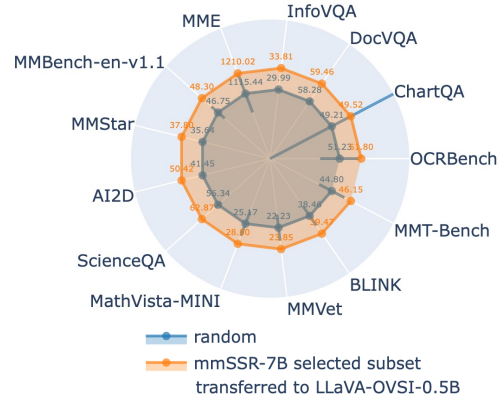


Figure 4. Transferability of mmSSR subsets: selected by mmSSR-7B, directly used to train a LLaVA-OVSI-0.5B variant.

MMVet (Yu et al., 2023), BLINK (Fu et al., 2024b), MMT-Bench (Ying et al., 2024), AI2D (Kembhavi et al., 2016), ScienceQA (Lu et al., 2022), MathVista_{MINI} (Lu et al., 2023). For the experiment in Sec. 4.4 that scales up in the OCR capability, we additionally evaluate mmSSR on OCR-Bench (Liu et al., 2023b), ChartQA (Masry et al., 2022), DocVQA (Mathew et al., 2021) and InfoVQA (Mathew et al., 2022). Since our setup focuses on the single-image SFT phase, the model does not possess the multi-image understanding ability. Thus, for MMMU and BLINK, we report results on the single-image QA split.

4.2. Main Results

mmSSR consistently outperform competitors across varying data budget and benchmarks. The comparative results on 10 multimodal benchmarks are presented in Tab. 1. It can be observed that whether the system is in a cold start (5% budget) or a warm start (30% budget) scenario, and regardless of the focus of the benchmark’s evaluation, the samples identified by our mmSSR consistently outperform random sampling in most cases, making it an excellent choice in real-world applications. In contrast, other comparative methods fail to surpass random sampling under most of the benchmarks. Specifically, the mid-stage model

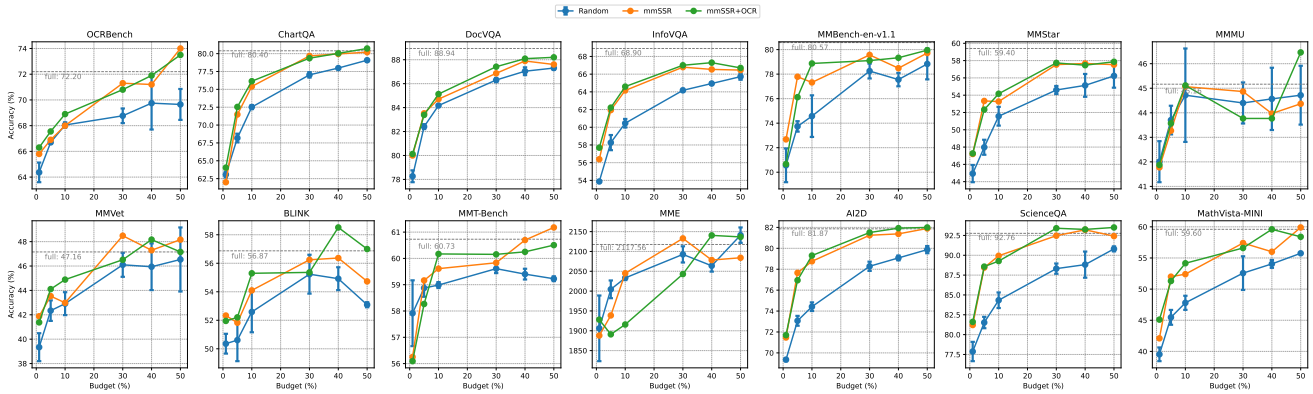


Figure 5. Results of scaling in data quantity (1% → 50%) and in data capability (basic 13 capabilities in mmSSR + new OCR samples).

of LLaVA-OV has not been instructed, hence the perplexity holds no referential significance. Although the SFT checkpoint LLaVA-OVSI shows marginally better performance, selecting samples with a fully fine-tuned model contradicts the motivation of the data selection task. Although the scorers of Deita (Liu et al., 2024b) have not been exposed to images, question-answer pairs should still aid in assessing sample value. However, results indicate that abstract criteria scoring like *quality* and *complexity* did not transfer well to the multi-modal task. While CLIP and E5-V can encode both modalities, experiments show that the emphasis of VLMs on image-text alignment is inconsistent with the optimization objectives of MLLMs. And COINCIDE (Lee et al., 2024), validated on LLaVA-1.5 (Liu et al., 2024a) and Vision-Flan (Xu et al., 2024), shows vulnerability to the 4× larger and shifted data pool.

Rich capabilities and styles guarantee the effectiveness of multi-modal data sampling. In Tab. 2, we compare our mmSSR with rich capabilities and styles, noted as mmSSR(ich), to the mmSSP(oor) variant where we simply query GPT-4o’s *quality* scores and corresponding explanations. In absence of style identification, we only improve diversity for mmSSP(oor) with image source during sampling. Results indicate that the abstract scoring criterion may introduce human-uninterpretable biases, which manifest as poor and inconsistent performance across different experimental settings and benchmarks.

Proxy mmSSR trained on GPT-4o judgments exhibit superior and more robust performance than open-source MLLM scoring. In this experiment, we investigate the necessity of proxy models. Given the same query for rich capability scores and styles, as well as the same diversity-aware score-prioritized selection strategy, our mmSSR(ich) fine-tunes proxy models to make predictions on the data pool, whereas mmSSR + Qwen2-VL and mmSSR + LLaVA-OVSI leverage their instruction following ability to directly

perform the scoring and styling task. As shown in Tab. 2, our specialized mmSSR still yields optimal performance, while utilizing our rich prompt to directly query Qwen2-VL also promises a stable improvement compared to random sampling. We note that our rich prompt combined with the SOTA open-source model delivers superior results compared to the baseline scoring task formulation paired with the advanced GPT-4o judgments. This further emphasizes the effectiveness of capability decomposition and style-based diversity sampling for the multi-modal data selection.

4.3. Transfer in Data Pool and Selection

Transfer mmSSR from shareGPT4v to LLaVA-OVSI. Common data curation scenarios often involve the addition of new subdomains. Here, we use 30% random subset of ShareGPT4v (Chen et al., 2024a) that consists of merely 12 sources (subdomains) as the base scenario to train mmSSR. These models are then directly generalize to LLaVA-OVSI (Li et al., 2024a) of 91 sources for inference and sampling. Results illustrated in Fig. 3 demonstrate strong generalization capability to the larger data pool with open sources and novel knowledge.

Transfer mmSSR selection to different model. We also expect the selected subset to be generally applicable, instead of being dependent on specific architecture or training settings (Munjal et al., 2020). To verify the effectiveness of the subset selected by mmSSR that are finetuned from LLaVA-OVSI-7B, we use it to train a 0.5B LLaVA-OVSI model. Results in Fig. 4 with 5% budget show that the superiority of our method remain, demonstrating strong robustness.

The superior performance of mmSSR can be attributed to the generality of the rich capabilities and styles we have articulated, which is effective across different model architectures, datasets, and validation settings. Specifically, *scores and styles are more generalizable than model responses*. While model-based methods rely on their specific

model responses (e.g., perplexity and embeddings) for data valuation, our mmSSR is instructed to score and identify instructional styles characterized by general semantics. Furthermore, *rich scores and styles are more generalizable than coarse-grained quality-like descriptors*. For pretrained MLLMs to be finetuned, while the understanding of quality might shift, the intrinsic knowledge of fine-grained capabilities and styles is more readily shared and transferable. Thus, the finetuned mmSSR and the selected subsets consistently guarantee strong and robust performance.

4.4. Scalability in Data Quantity and Capability

We further validated the scalability of the proposed mmSSR under varying data volumes in both colder-start (1%) and hot-start (40%, 50%) scenarios, achieving consistently superior MLLM performance, as shown in Fig. 5. Beyond quantity, we consider a data expansion scenario commonly encountered in real-world applications, scaling up the capability dimension within the existing data pool. Taking OCR as an example, we query GPT-4o for judgments on it and fine-tune mmSSR to select highly-scored OCR samples. The newly added samples lead to steady improvements in OCR-related benchmarks. Furthermore, they contribute to the growth of general benchmarks or sustain their advantageous positions, demonstrating great scalability.

5. Conclusion

As the first multi-modal data selection method for SOTA MLLMs, mmSSR leverages the nature of instruction tuning to decompose multi-modal data into capability scores and interaction styles and make judgment over those proxies. On the one hand, it facilitates diversity-aware score-prioritized sampling, demonstrating superior performance across 14 benchmarks and 6 budget settings. On the other hand, the formulation of concrete quality criteria with semantics guarantees capability customization and strong generalizability. Our diversity indicator supports efficient scaling, which promises broad applicability and accessibility.

Impact Statement

This paper presents work whose goal is to advance the field of Machine Learning. There are many potential societal consequences of our work, none which we feel must be specifically highlighted here.

References

Achiam, J., Adler, S., Agarwal, S., Ahmad, L., Akkaya, I., Aleman, F. L., Almeida, D., Altenschmidt, J., Altman, S., Anadkat, S., et al. Gpt-4 technical report. *arXiv preprint arXiv:2303.08774*, 2023.

Brown, T., Mann, B., Ryder, N., Subbiah, M., Kaplan, J. D., Dhariwal, P., Neelakantan, A., Shyam, P., Sastry, G., Askell, A., et al. Language models are few-shot learners. *Advances in neural information processing systems*, 33: 1877–1901, 2020.

Chen, L., Li, J., Dong, X., Zhang, P., He, C., Wang, J., Zhao, F., and Lin, D. Sharegpt4v: Improving large multi-modal models with better captions. In *European Conference on Computer Vision*, pp. 370–387. Springer, 2024a.

Chen, L., Li, J., Dong, X., Zhang, P., Zang, Y., Chen, Z., Duan, H., Wang, J., Qiao, Y., Lin, D., et al. Are we on the right way for evaluating large vision-language models? *arXiv preprint arXiv:2403.20330*, 2024b.

Chung, H. W., Hou, L., Longpre, S., Zoph, B., Tay, Y., Fedus, W., Li, Y., Wang, X., Dehghani, M., Brahma, S., et al. Scaling instruction-finetuned language models. *Journal of Machine Learning Research*, 25(70):1–53, 2024.

Diddee, H. and Ippolito, D. Chasing Random: Instruction Selection Strategies Fail to Generalize, October 2024.

Duan, H., Yang, J., Qiao, Y., Fang, X., Chen, L., Liu, Y., Dong, X., Zang, Y., Zhang, P., Wang, J., et al. Vlmevalkit: An open-source toolkit for evaluating large multi-modality models. In *Proceedings of the 32nd ACM International Conference on Multimedia*, pp. 11198–11201, 2024.

Dubey, A., Jauhri, A., Pandey, A., Kadian, A., Al-Dahle, A., Letman, A., Mathur, A., Schelten, A., Yang, A., Fan, A., Goyal, A., Hartshorn, A., Yang, A., Mitra, A., Sravankumar, A., Korenev, A., Hinsvark, A., Rao, A., Zhang, A., Rodriguez, A., Gregerson, A., Spataru, A., Roziere, B., Biron, B., Tang, B., Chern, B., Caucheteux, C., Nayak, C., Bi, C., Marra, C., McConnell, C., Keller, C., Touret, C., Wu, C., Wong, C., Ferrer, C. C., Nikolaidis, C., Al-lonsius, D., Song, D., Pintz, D., Livshits, D., Esiobu, D., Choudhary, D., Mahajan, D., Garcia-Olano, D., Perino, D., Hupkes, D., Lakomkin, E., AlBadawy, E., Lobanova, E., Dinan, E., Smith, E. M., Radenovic, F., Zhang, F., Synnaeve, G., Lee, G., Anderson, G. L., Nail, G., Mialon, G., Pang, G., Cucurell, G., Nguyen, H., Korevaar, H., Xu, H., Touvron, H., Zarov, I., Ibarra, I. A., Kloumann, I., Misra, I., Evtimov, I., Copet, J., Lee, J., Geffert, J., Vranes, J., Park, J., Mahadeokar, J., Shah, J., van der Linde, J., Billock, J., Hong, J., Lee, J., Fu, J., Chi, J., Huang, J., Liu, J., Wang, J., Yu, J., Bitton, J., Spisak, J., Park, J., Rocca, J., Johnston, J., Saxe, J., Jia, J., Alwala, K. V., Upasani, K., Plawiak, K., Li, K., Heafield, K., Stone, K., El-Arini, K., Iyer, K., Malik, K., Chiu, K., Bhalla, K., Rantala-Yeary, L., van der Maaten, L., Chen, L., Tan, L., Jenkins, L., Martin, L., Madaan, L., Malo, L., Blecher, L., Landzaat, L., de Oliveira, L., Muzzi, M., Pasupuleti, M., Singh, M.,

- Paluri, M., Kardas, M., Oldham, M., Rita, M., Pavlova, M., Kambadur, M., Lewis, M., Si, M., Singh, M. K., Hassan, M., Goyal, N., Torabi, N., Bashlykov, N., Bogoychev, N., Chatterji, N., Duchenne, O., Çelebi, O., Alrassy, P., Zhang, P., Li, P., Vasic, P., Weng, P., Bhargava, P., Dubal, P., Krishnan, P., Koura, P. S., Xu, P., He, Q., Dong, Q., Srinivasan, R., Ganapathy, R., Calderer, R., Cabral, R. S., Stojnic, R., Raileanu, R., Girdhar, R., Patel, R., Sauvestre, R., Polidoro, R., Sumbaly, R., Taylor, R., Silva, R., Hou, R., Wang, R., Hosseini, S., Chennabasappa, S., Singh, S., Bell, S., Kim, S. S., Edunov, S., Nie, S., Narang, S., Rapparth, S., Shen, S., Wan, S., Bhosale, S., Zhang, S., Vandenhende, S., Batra, S., Whitman, S., Sootla, S., Collot, S., Gururangan, S., Borodinsky, S., Herman, T., Fowler, T., Sheasha, T., Georgiou, T., Scialom, T., Speckbacher, T., Mihaylov, T., Xiao, T., Karn, U., Goswami, V., Gupta, V., Ramanathan, V., Kerkez, V., Gonguet, V., Do, V., Vogeti, V., Petrovic, V., Chu, W., Xiong, W., Fu, W., Meers, W., Martinet, X., Wang, X., Tan, X. E., Xie, X., Jia, X., Wang, X., Goldschlag, Y., Gaur, Y., Babaei, Y., Wen, Y., Song, Y., Zhang, Y., Li, Y., Mao, Y., Coudert, Z. D., Yan, Z., Chen, Z., Papakipos, Z., Singh, A., Grattafiori, A., Jain, A., Kelsey, A., Shajnfeld, A., Gangidi, A., Victoria, A., Goldstand, A., Menon, A., Sharma, A., Boesenberg, A., Vaughan, A., Baevski, A., Feinstein, A., Kallet, A., Sangani, A., Yunus, A., Lupu, A., Alvarado, A., Caples, A., Gu, A., Ho, A., Poulton, A., Ryan, A., Ramchandani, A., Franco, A., Saraf, A., Chowdhury, A., Gabriel, A., Bharambe, A., Eisenman, A., Yazdan, A., James, B., Maurer, B., Leonhardi, B., Huang, B., Loyd, B., De Paola, B., Paranjape, B., Liu, B., Wu, B., Ni, B., Hancock, B., Wasti, B., Spence, B., Stojkovic, B., Gamido, B., Montalvo, B., Parker, C., Burton, C., Mejia, C., Wang, C., Kim, C., Zhou, C., Hu, C., Chu, C.-H., Cai, C., Tindal, C., Feichtenhofer, C., Civin, D., Beaty, D., Kreymer, D., Li, D., Wyatt, D., Adkins, D., Xu, D., Testuggine, D., David, D., Parikh, D., Liskovich, D., Foss, D., Wang, D., Le, D., Holland, D., Dowling, E., Jamil, E., Montgomery, E., Presani, E., Hahn, E., Wood, E., Brinkman, E., Arcaute, E., Dunbar, E., Smothers, E., Sun, F., Kreuk, F., Tian, F., Ozgenel, F., Caggioni, F., Guzmán, F., Kanayet, F., Seide, F., Florez, G. M., Schwarz, G., Badeer, G., Swee, G., Halpern, G., Thattai, G., Herman, G., Sizov, G., Guangyi, Zhang, Lakshminarayanan, G., Shojanazeri, H., Zou, H., Wang, H., Zha, H., Habeeb, H., Rudolph, H., Suk, H., Aspegren, H., Goldman, H., Damraj, I., Molybog, I., Tufanov, I., Veliche, I.-E., Gat, I., Weissman, J., Geboski, J., Kohli, J., Asher, J., Gaya, J.-B., Marcus, J., Tang, J., Chan, J., Zhen, J., Reizenstein, J., Teboul, J., Zhong, J., Jin, J., Yang, J., Cummings, J., Carvill, J., Shepard, J., McPhie, J., Torres, J., Ginsburg, J., Wang, J., Wu, K., U, K. H., Saxena, K., Prasad, K., Khandelwal, K., Zand, K., Matosich, K., Veeraghavan, K., Michelena, K., Li, K., Huang, K., Chawla, K., Lakhotia, K., Huang, K., Chen, L., Garg, L., A, L., Silva, L., Bell, L., Zhang, L., Guo, L., Yu, L., Moshkovich, L., Wehrstedt, L., Khabsa, M., Avalani, M., Bhatt, M., Tsimpoukelli, M., Mankus, M., Hasson, M., Lennie, M., Reso, M., Groshev, M., Naumov, M., Lathi, M., Keneally, M., Seltzer, M. L., Valko, M., Restrepo, M., Patel, M., Vyatskov, M., Samvelyan, M., Clark, M., Macey, M., Wang, M., Hermoso, M. J., Metanat, M., Rastegari, M., Bansal, M., Santhanam, N., Parks, N., White, N., Bawa, N., Singhal, N., Egebo, N., Usunier, N., Laptev, N. P., Dong, N., Zhang, N., Cheng, N., Chernoguz, O., Hart, O., Salpekar, O., Kalinli, O., Kent, P., Parekh, P., Saab, P., Balaji, P., Rittner, P., Bontrager, P., Roux, P., Dollar, P., Zvyagina, P., Ratanchandani, P., Yuvraj, P., Liang, Q., Alao, R., Rodriguez, R., Ayub, R., Murthy, R., Nayani, R., Mitra, R., Li, R., Hogan, R., Battey, R., Wang, R., Maheswari, R., Howes, R., Rinott, R., Bondu, S. J., Datta, S., Chugh, S., Hunt, S., Dhillon, S., Sidorov, S., Pan, S., Verma, S., Yamamoto, S., Ramaswamy, S., Lindsay, S., Lindsay, S., Feng, S., Lin, S., Zha, S. C., Shankar, S., Zhang, S., Zhang, S., Wang, S., Agarwal, S., Sajuyigbe, S., Chintala, S., Max, S., Chen, S., Kehoe, S., Satterfield, S., Govindaprasad, S., Gupta, S., Cho, S., Virk, S., Subramanian, S., Choudhury, S., Goldman, S., Remez, T., Glaser, T., Best, T., Kohler, T., Robinson, T., Li, T., Zhang, T., Matthews, T., Chou, T., Shaked, T., Vontimitta, V., Ajayi, V., Montanez, V., Mohan, V., Kumar, V. S., Mangla, V., Albiero, V., Ionescu, V., Poenaru, V., Mihailescu, V. T., Ivanov, V., Li, W., Wang, W., Jiang, W., Bouaziz, W., Constable, W., Tang, X., Wang, X., Wu, X., Wang, X., Xia, X., Wu, X., Gao, X., Chen, Y., Hu, Y., Jia, Y., Qi, Y., Li, Y., Zhang, Y., Zhang, Y., Adi, Y., Nam, Y., Yu, Wang, Hao, Y., Qian, Y., He, Y., Rait, Z., DeVito, Z., Rosnbrick, Z., Wen, Z., Yang, Z., and Zhao, Z. *The Llama 3 Herd of Models*, August 2024.
- Elazar, Y., Bhagia, A., Magnusson, I. H., Ravichander, A., Schwenk, D., Suhr, A., Walsh, E. P., Groeneveld, D., Soldaini, L., Singh, S., et al. What's in my big data? In *The Twelfth International Conference on Learning Representations*, 2024.
- Evans, T., Pathak, S., Merzic, H., Schwarz, J., Tanno, R., and Henaff, O. J. Bad Students Make Great Teachers: Active Learning Accelerates Large-Scale Visual Understanding, February 2024.
- Fu, C., Chen, P., Shen, Y., Qin, Y., Zhang, M., Lin, X., Yang, J., Zheng, X., Li, K., Sun, X., Wu, Y., and Ji, R. Mme: A comprehensive evaluation benchmark for multimodal large language models, 2024a. URL <https://arxiv.org/abs/2306.13394>.
- Fu, X., Hu, Y., Li, B., Feng, Y., Wang, H., Lin, X., Roth, D., Smith, N. A., Ma, W.-C., and Krishna, R. Blink: Multimodal large language models can see but not perceive. *arXiv preprint arXiv:2404.12390*, 2024b.

- Gadre, S. Y., Ilharco, G., Fang, A., Hayase, J., Smyrnis, G., Nguyen, T., Marten, R., Wortsman, M., Ghosh, D., Zhang, J., Orgad, E., Entezari, R., Daras, G., Pratt, S., Ramanujan, V., Bitton, Y., Marathe, K., Musmann, S., Vencu, R., Cherti, M., Krishna, R., Koh, P. W., Saukh, O., Ratner, A., Song, S., Hajishirzi, H., Farhadi, A., Beaumont, R., Oh, S., Dimakis, A., Jitsev, J., Carmon, Y., Shankar, V., and Schmidt, L. DataComp: In search of the next generation of multimodal datasets. In *Thirty-Seventh Conference on Neural Information Processing Systems Datasets and Benchmarks Track*, October 2023.
- Gao, T., Wettig, A., He, L., Dong, Y., Malladi, S., and Chen, D. Metadata Conditioning Accelerates Language Model Pre-training, January 2025.
- Goyal, S., Maini, P., Lipton, Z. C., Raghunathan, A., and Kolter, J. Z. Scaling Laws for Data Filtering – Data Curation cannot be Compute Agnostic. In *Proceedings of the IEEE/CVF Conference on Computer Vision and Pattern Recognition (CVPR)*, pp. 22702–22711, April 2024.
- Jiang, T., Song, M., Zhang, Z., Huang, H., Deng, W., Sun, F., Zhang, Q., Wang, D., and Zhuang, F. E5-V: Universal Embeddings with Multimodal Large Language Models, July 2024.
- Joulin, A. Fasttext. zip: Compressing text classification models. *arXiv preprint arXiv:1612.03651*, 2016.
- Kembhavi, A., Salvato, M., Kolve, E., Seo, M., Hajishirzi, H., and Farhadi, A. A diagram is worth a dozen images. In *Computer Vision—ECCV 2016: 14th European Conference, Amsterdam, The Netherlands, October 11–14, 2016, Proceedings, Part IV 14*, pp. 235–251. Springer, 2016.
- Lee, J., Li, B., and Hwang, S. J. Concept-skill transferability-based data selection for large vision-language models. In *Proceedings of the 2024 Conference on Empirical Methods in Natural Language Processing*, pp. 5060–5080, 2024.
- Lee, K., Ippolito, D., Nystrom, A., Zhang, C., Eck, D., Callison-Burch, C., and Carlini, N. Deduplicating training data makes language models better. In *Proceedings of the 60th Annual Meeting of the Association for Computational Linguistics (Volume 1: Long Papers)*, pp. 8424–8445, 2022.
- Li, B., Zhang, Y., Guo, D., Zhang, R., Li, F., Zhang, H., Zhang, K., Li, Y., Liu, Z., and Li, C. LLaVA-OneVision: Easy Visual Task Transfer, August 2024a.
- Li, J., Fang, A., Smyrnis, G., Ivgi, M., Jordan, M., Gadre, S., Bansal, H., Guha, E., Keh, S., Arora, K., Garg, S., Xin, R., Muennighoff, N., Heckel, R., Mercat, J., Chen, M., Gururangan, S., Wortsman, M., Albalak, A., Bitton, Y., Nezhurina, M., Abbas, A., Hsieh, C.-Y., Ghosh, D., Gardner, J., Kilian, M., Zhang, H., Shao, R., Pratt, S., Sanyal, S., Ilharco, G., Daras, G., Marathe, K., Gokaslan, A., Zhang, J., Chandu, K., Nguyen, T., Vasiljevic, I., Kakade, S., Song, S., Sanghavi, S., Faghri, F., Oh, S., Zettlemoyer, L., Lo, K., El-Nouby, A., Pouransari, H., Toshev, A., Wang, S., Groeneveld, D., Soldaini, L., Koh, P. W., Jitsev, J., Kollar, T., Dimakis, A. G., Carmon, Y., Dave, A., Schmidt, L., and Shankar, V. DataComp-LM: In search of the next generation of training sets for language models, June 2024b.
- Li, M., Zhang, Y., Li, Z., Chen, J., Chen, L., Cheng, N., Wang, J., Zhou, T., and Xiao, J. From Quantity to Quality: Boosting LLM Performance with Self-Guided Data Selection for Instruction Tuning. In *Proceedings of the 2024 Conference of the North American Chapter of the Association for Computational Linguistics: Human Language Technologies (Volume 1: Long Papers)*, pp. 7595–7628, April 2024c.
- Liu, H., Li, C., Li, Y., and Lee, Y. J. Improved baselines with visual instruction tuning. In *Proceedings of the IEEE/CVF Conference on Computer Vision and Pattern Recognition*, pp. 26296–26306, 2024a.
- Liu, L., Liu, X., Wong, D. F., Li, D., Wang, Z., Hu, B., and Zhang, M. SelectIT: Selective Instruction Tuning for LLMs via Uncertainty-Aware Self-Reflection. In *The Thirty-eighth Annual Conference on Neural Information Processing Systems*, January 2025.
- Liu, W., Zeng, W., He, K., Jiang, Y., and He, J. What Makes Good Data for Alignment? A Comprehensive Study of Automatic Data Selection in Instruction Tuning. In *The Twelfth International Conference on Learning Representations*, 2024b.
- Liu, Y., Duan, H., Zhang, Y., Li, B., Zhang, S., Zhao, W., Yuan, Y., Wang, J., He, C., and Liu, Z. Mmbench: Is your multi-modal model an all-around player? *Technical Report*, 2023a.
- Liu, Y., Li, Z., Yang, B., Li, C., Yin, X., Liu, C.-l., Jin, L., and Bai, X. On the hidden mystery of ocr in large multimodal models. *arXiv preprint arXiv:2305.07895*, 2023b.
- Liu, Z., Zhou, K., Zhao, W. X., Gao, D., Li, Y., and Wen, J.-R. Less is More: High-value Data Selection for Visual Instruction Tuning, October 2024c.
- Lu, K., Yuan, H., Yuan, Z., Lin, R., Lin, J., Tan, C., Zhou, C., and Zhou, J. #INSTAG: INSTRUCTION TAGGING FOR ANALYZING SUPERVISED FINE-TUNING OF

- LARGE LANGUAGE MODELS. In *The Twelfth International Conference on Learning Representations* The Twelfth International Conference on Learning Representations, March 2024.
- Lu, P., Mishra, S., Xia, T., Qiu, L., Chang, K.-W., Zhu, S.-C., Tafjord, O., Clark, P., and Kalyan, A. Learn to explain: Multimodal reasoning via thought chains for science question answering. In *The 36th Conference on Neural Information Processing Systems (NeurIPS)*, 2022.
- Lu, P., Bansal, H., Xia, T., Liu, J., Li, C., Hajishirzi, H., Cheng, H., Chang, K.-W., Galley, M., and Gao, J. Mathvista: Evaluating math reasoning in visual contexts with gpt-4v, bard, and other large multimodal models. *arXiv preprint arXiv:2310.02255*, 2023.
- Luo, G., Yang, X., Dou, W., Wang, Z., Liu, J., Dai, J., Qiao, Y., and Zhu, X. Mono-InternVL: Pushing the Boundaries of Monolithic Multimodal Large Language Models with Endogenous Visual Pre-training, November 2024.
- Lyu, M., Zhou, J., Chen, H., Huang, Y., Yu, D., Li, Y., Guo, Y., Guo, Y., Xiang, L., and Ding, G. Box-level active detection. In *Proceedings of the IEEE/CVF Conference on Computer Vision and Pattern Recognition*, pp. 23766–23775, 2023.
- Lyu, M., Hao, T., Xu, X., Chen, H., Lin, Z., Han, J., and Ding, G. Learn from the learnt: source-free active domain adaptation via contrastive sampling and visual persistence. In *European Conference on Computer Vision*, pp. 228–246. Springer, 2025.
- Maini, P., Goyal, S., Lipton, Z. C., Kolter, J. Z., and Raghunathan, A. T-MARS: Improving Visual Representations by Circumventing Text Feature Learning, March 2024.
- Masry, A., Long, D. X., Tan, J. Q., Joty, S., and Hoque, E. Chartqa: A benchmark for question answering about charts with visual and logical reasoning. In *ACL*, 2022.
- Mathew, M., Karatzas, D., and Jawahar, C. Docvqa: A dataset for vqa on document images. In *WACV*, 2021.
- Mathew, M., Bagal, V., Tito, R., Karatzas, D., Valveny, E., and Jawahar, C. Infographicvqa. In *Proceedings of the IEEE/CVF Winter Conference on Applications of Computer Vision*, pp. 1697–1706, 2022.
- Munjal, P., Hayat, N., Hayat, M., Sourati, J., and Khan, S. Towards Robust and Reproducible Active Learning Using Neural Networks. In *Proceedings of the IEEE/CVF Conference on Computer Vision and Pattern Recognition (CVPR)*, pp. 223–232, 2020.
- Pang, J., Wei, J., Shah, A. P., Zhu, Z., Wang, Y., Qian, C., Liu, Y., Bao, Y., and Wei, W. Improving data efficiency via curating llm-driven rating systems. *arXiv preprint arXiv:2410.10877*, 2024.
- Penedo, G., Malartic, Q., Hesslow, D., Cojocaru, R., Cappelli, A., Alobeidli, H., Pannier, B., Almazrouei, E., and Launay, J. The refinedweb dataset for falcon llm: outperforming curated corpora with web data, and web data only. *arXiv preprint arXiv:2306.01116*, 2023.
- Qin, Y., Yang, Y., Guo, P., Li, G., Shao, H., Shi, Y., Xu, Z., Gu, Y., Li, K., and Sun, X. Unleashing the Power of Data Tsunami: A Comprehensive Survey on Data Assessment and Selection for Instruction Tuning of Language Models. *Transactions on Machine Learning Research*, December 2024.
- Radford, A., Kim, J. W., Hallacy, C., Ramesh, A., Goh, G., Agarwal, S., Sastry, G., Askell, A., Mishkin, P., Clark, J., et al. Learning transferable visual models from natural language supervision. In *International conference on machine learning*, pp. 8748–8763. PMLR, 2021.
- Sener, O. and Savarese, S. Active learning for convolutional neural networks: A core-set approach. In *International Conference on Learning Representations*, 2018.
- Settles, B. Active learning literature survey. Computer Sciences Technical Report 1648, University of Wisconsin-Madison, 2009.
- Team, G., Anil, R., Borgeaud, S., Alayrac, J.-B., Yu, J., Soricut, R., Schalkwyk, J., Dai, A. M., Hauth, A., Millican, K., et al. Gemini: a family of highly capable multimodal models. *arXiv preprint arXiv:2312.11805*, 2023.
- Team, G., Riviere, M., Pathak, S., Sessa, P. G., Hardin, C., Bhupatiraju, S., Hussenot, L., Mesnard, T., Shahriari, B., Ramé, A., et al. Gemma 2: Improving open language models at a practical size. *arXiv preprint arXiv:2408.00118*, 2024.
- Touvron, H., Lavril, T., Izacard, G., Martinet, X., Lachaux, M.-A., Lacroix, T., Rozière, B., Goyal, N., Hambro, E., Azhar, F., et al. Llama: Open and efficient foundation language models. *arXiv preprint arXiv:2302.13971*, 2023.
- Wang, A., Chen, H., Tan, J., Zhang, K., Cai, X., Lin, Z., Han, J., and Ding, G. Prefixkv: Adaptive prefix kv cache is what vision instruction-following models need for efficient generation. *arXiv preprint arXiv:2412.03409*, 2024a.
- Wang, P., Bai, S., Tan, S., Wang, S., Fan, Z., Bai, J., Chen, K., Liu, X., Wang, J., Ge, W., Fan, Y., Dang, K., Du, M., Ren, X., Men, R., Liu, D., Zhou, C., Zhou, J., and Lin, J. Qwen2-vl: Enhancing vision-language model’s perception of the world at any resolution. *arXiv preprint arXiv:2409.12191*, 2024b.

- Wang, T., Kulikov, I., Golovneva, O., Yu, P., Yuan, W., Dwivedi-Yu, J., Pang, R. Y., Fazel-Zarandi, M., Weston, J., and Li, X. Self-Taught Evaluators, August 2024c.
- Wettig, A., Gupta, A., Malik, S., and Chen, D. QuRating: Selecting High-Quality Data for Training Language Models. In *International Conference on Machine Learning (ICML)*, July 2024.
- Xia, M., Malladi, S., Gururangan, S., Arora, S., and Chen, D. LESS: Selecting Influential Data for Targeted Instruction Tuning. In *Forty-First International Conference on Machine Learning*, June 2024a.
- Xia, T., Yu, B., Dang, K., Yang, A., Wu, Y., Tian, Y., Chang, Y., and Lin, J. Rethinking Data Selection at Scale: Random Selection is Almost All You Need, December 2024b.
- Xu, Y., Yao, Y., Huang, Y., Qi, M., Wang, M., Gu, B., and Sundaresan, N. Rethinking the instruction quality: Lift is what you need. *CoRR*, 2023.
- Xu, Z., Feng, C., Shao, R., Ashby, T., Shen, Y., Jin, D., Cheng, Y., Wang, Q., and Huang, L. Vision-flan: Scaling human-labeled tasks in visual instruction tuning. In *Findings of the Association for Computational Linguistics ACL 2024*, pp. 15271–15342, 2024.
- Ying, K., Meng, F., Wang, J., Li, Z., Lin, H., Yang, Y., Zhang, H., Zhang, W., Lin, Y., Liu, S., Lei, J., Lu, Q., Chen, R., Xu, P., Zhang, R., Zhang, H., Gao, P., Wang, Y., Qiao, Y., Luo, P., Zhang, K., and Shao, W. Mmt-bench: A comprehensive multimodal benchmark for evaluating large vision-language models towards multitask agi, 2024.
- Yu, W., Yang, Z., Li, L., Wang, J., Lin, K., Liu, Z., Wang, X., and Wang, L. Mm-vet: Evaluating large multimodal models for integrated capabilities, 2023. URL <https://arxiv.org/abs/2308.02490>.
- Yuan, W., Pang, R. Y., Cho, K., Li, X., Sukhbaatar, S., Xu, J., and Weston, J. Self-Rewarding Language Models. In *Forty-First International Conference on Machine Learning*, May 2024.
- Yue, X., Ni, Y., Zhang, K., Zheng, T., Liu, R., Zhang, G., Stevens, S., Jiang, D., Ren, W., and Sun, Y. Mmmu: A massive multi-discipline multimodal understanding and reasoning benchmark for expert agi. In *CVPR*, 2024.
- Zhou, C., Liu, P., Xu, P., Iyer, S., Sun, J., Mao, Y., Ma, X., Efrat, A., Yu, P., Yu, L., et al. Lima: Less is more for alignment. *Advances in Neural Information Processing Systems*, 36, 2024.
- Zhou, D., Wang, K., Gu, J., Peng, X., Lian, D., Zhang, Y., You, Y., and Feng, J. Dataset quantization. In *Proceedings of the IEEE/CVF International Conference on Computer Vision*, pp. 17205–17216, 2023.

A. Additional Setup Details

A.1. Capabilities and Styles

Tab. 3 presents capabilities and interaction styles that we determine can contribute to building a comprehensive and general-purpose MLLM, which are present in the current open-access data pool. During the initial exploration, we provided initially derived candidates and inspired GPT-4o to identify new patterns. After two iterations of optimization, the final list was established. Beyond abstract criteria such as quality and rarity adopted by previous research (Liu et al., 2024b; Pang et al., 2024), our rich capabilities cover various levels of granularity, ranging from general information valuation (e.g., attribute) to specialized knowledge identification (e.g., STEM), with varying prevalence.

As publicly collected data becomes more abundant or when sampling from private specialized datasets, our mmSSR pipeline can be effectively applied to a wider range of contexts to extract new knowledge, such as image-based creative writing, chain-of-thought reasoning, competition problem-solution math problem etc.

Table 3: 14 criteria we recognize as the foundational pillars for developing vision perception and reasoning capabilities within MLLMs, and the interaction styles we identify from instructional multi-modal data.

CAPABILITY	DEFINITION	EXAMPLES
activity recognition	actions or behaviors of humans, animals, or objects	Fig. 13
causal reasoning	cause-and-effect relationships between events or variables to predict outcomes and explain phenomena	Fig. 14
humanities	history, literature, philosophy, art, and culture to understand human experiences and societal developments	Fig. 15
STEM knowledge	science, technology, engineering, and mathematics, chemistry, economics etc	Fig. 16
comparative analysis	compare multiple entities, concepts, or datasets to identify similarities, differences, and relationships	Fig. 17
data understanding	documents, tables, charts, graphics, infographics	Fig. 18
object spatial understanding	the positions, orientations, countings and relationships of objects	Fig. 19
attribute identification	various characteristics and properties of objects, such as identity, color, size, shape, material, emotion, and other distinguishing features	Fig. 20
logical deduction	to analyze information, recognize patterns, draw valid conclusions based on structured principles of logic and make reasoned decisions	Fig. 21
scene understanding	complex environment with objects, their attributes, spatial relationships, and activities, as well as surrounding information and circumstances within the scene	Fig. 22
fine-grained recognition	subtle differences and specific features within similar categories of objects	Fig. 23
language generation	generate coherent and contextually appropriate text in various languages, styles, and formats based on instructions	Fig. 24
in-context learning	follow the demonstrations of the task within a given conversation	Fig. 25
optical character recognition	the conversion between images of printed/handwritten text and machine-readable text	Fig. 26
style	multi-choice, coordinate, yes/no, word/short-phrase, short description, detailed description, comparison, chain-of-thought (step-by-step), specified style	Fig. 13-26

A.2. Prompt Template for Rich Scores and Styles

Below gives our query template, where [Input] and [Response] are paired questions and answers. Multi-round user-assistant interactions are concatenated for demonstration. To enhance the stability of pointwise scoring of by GPT-4o, we define

a score scale from 0 to 5 and establish clear benchmarks. Each data sample is evaluated on all capability dimensions, querying scores and recalling all observed styles in the text modality. To improve the self-consistency of responses, we require explanations for the given scores. Particularly, in the valuation of multi-modal data, we emphasize the importance of balancing the correlation between image and text modalities in task-specific contexts, i.e., scoring and styling, rather than allowing the model to be biased towards a single modality, such as being dominated by language or vision.

To examine the effectiveness of our prompt and the quality of GPT-4o judgment, for each capability, we present examples scored 0-5 in Fig. 13-Fig. 26, accompanied by detailed explanations. We note that when obtaining costly human scoring is impractical, using ChatGPT could introduce hallucinations (e.g., 3rd example in Fig. 24, 4th example in Fig. 25). However, it still serves as a viable sub gold standard. Take the 3rd and 5th samples in Fig. 26 for example. Although the visual content in these scenes is similar, the text queries focus on distinct elements. When the task requires generating an “informative summary” and the answer is related to reading text on a vehicle, the contribution of this training sample to the OCR capability is crucial, yielding a score of 3. Conversely, when the task shifts to global scene understanding with an emphasis on road details, the background text in the 5th image becomes irrelevant, resulting in a score of 0. Hallucinations present in the original samples within the answers, such as the 4th example in Fig. 19, can also be identified and thus given lower scores, preventing the propagation of incorrect information in subsequent SFT processes. These cases demonstrate the efficiency of prompt instructions, highlighting that the balance between image-query-task in data curation meets expectations.

Prompt to Query GPT-4o for Rich Scores and Styles

System Prompt:

You are an AI expert rater designed to analyze the Visual Question Answering (VQA) instance in the user query to perform the following tasks step-by-step:

Step 1: Classify the VQA instance into given conversation style.

Step 2: Evaluate the helpfulness of the information provided in the VQA instance with respect to various model capabilities. Specifically, rate how well this information could enhance each capability of a multi-modal large language model through learning from it.

Step 3: Output the results strictly follow the JSON format.

User Prompt:

Instruction

You need to perform the following three steps to rate the User Query and output result in the dictionary format.

Step 1: Classify the instance in interaction style. Determine the task style of the VQA instance and select styles from the list “task_styles” below. Sort the selected styles by frequency of occurrence.

Step 2: Rate each capability from 0-5. For each capability listed and explained in “task_capabilities” below, analyze how effectively the VQA instance could enhance that capability of a Multimodal Large Language Model (MLLM) by learning from it. Rate each capability using the scores from the “score_scale” list below in reference to the guidelines. Please ensure that the scores are well-distributed across the range.

Finally, output the results strictly following the dictionary format defined in Output Format. Do not output any additional tokens outside it.

User Query

Question: [Input]

Answer: [Response]

Task Styling

```
task_styles = [
    multi-choice,
    coordinate,
    ... # See Tab. 3 for the full list
]
```

Prompt to Query GPT-4o for Rich Scores and Styles

```

## Task Capabilities
task_capabilities = [
    optical character recognition, # the conversion between images of printed/handwritten text and machine-
    readable text
    ... # See Tab. 3 for the full list and explanation
]

## Rating Scale
score_scale = [
    0, # Not Relevant: The VQA instance does not present or relate to the capability in any meaningful way.
    1, # Minimal: The VQA instance offers very little information relevant to the capability, providing negligible
    value for enhancement.
    2, # Fair: The VQA instance contains some relevant information but lacks depth and clarity, contributing
    minimally to the model's learning in this capability.
    3, # Good: The VQA instance provides a fair amount of relevant information, which can moderately aid in
    the model's learning and enhancement of the capability.
    4, # Significant: The VQA instance offers substantial information that is highly relevant and beneficial,
    significantly aiding the model's learning and enhancement of the capability.
    5, # Excellent: The VQA instance is exceptionally rich in relevant information, providing comprehensive
    and clear insights that would greatly enhance the model's learning and mastery of the capability.
]

## Output Format
{
    "style": "<list of string>",
    "capability2score": "<dict of str:int>",
    "capability2explanation": "<dict of str:str>",
}

```

B. Validation on Benchmark Test Splits

We compared the baselines and our mmSSR across various selection settings within a unified framework, obtaining batches of results. The intra-batch comparison of results is sufficient to validate the effectiveness of sampling strategies. Thus, considering the limitations on the number of evaluations in the online assessment system, we primarily report the results of MMBench_{en-v1.1} (Liu et al., 2023a), MMMU (Yue et al., 2024), and MMT-Bench (Ying et al., 2024) on their validation set in Tab. 1. We then select the top samplers for submission to the online test split, with the results presented in Table 4.

Similar to the main experiment, our comparative results on the test split consistently outperform or match the performance of SOTA baselines. In addition to maintaining a stable absolute advantage regardless of the data budget, mmSSR exhibits particularly remarkable effectiveness during the challenging cold phase. Without dependency on pre-trained model features or pre-selected hyperparameters, our semantic-based rich capabilities and superficial styles show stronger transferability to the test sets. Besides, the trends and the full performance observed in the MMMU dataset indicate that the task remains challenging for the current single-image data pool. To achieve further improvements, it would be beneficial to integrate additional external data that includes college-level multidisciplinary knowledge.

C. Validation of Scorer and Styler Predictions

C.1. Error Analysis of Scorers

The training of Scorers and Styler follows the original instructional tuning strategy under the LLaVA-OVSI frameworks (Li et al., 2024a)⁵. To minimize the exploration cost of mmSSR in practical applications, no hyperparameter fine-tuning is

⁵https://github.com/LLaVA-VL/LLaVA-NeXT/blob/main/scripts/train/finetune_si.sh

Table 4. Performance comparison on the benchmarks with online test splits conducted across varying budgets of 5%, 10% and 30% of LLaVA-OVSI. We highlight the best result in **boldface** and underline the result if it beats the random baseline. The column >Rand presents the number of benchmarks where the method exceeds random sampling, and /FULL compares the performance of sampled data with that of the FULL dataset.

	MMBench _{ne-v1.1-test}	MMMU _{test}	MMT-Bench _{all}	>Rand	/FULL
Budget: 5%					
Random	73.45	40.37	59.98	-	96.32%
Deita	<u>73.97</u>	36.30	56.57	1/3	91.40%
COINCIDE	<u>73.09</u>	40.30	57.47	0/3	94.74%
mmSSR	<u>75.84</u>	<u>41.30</u>	<u>60.10</u>	3/3	<u>98.15%</u>
Budget: 10%					
Random	74.55	40.40	60.54	-	97.12%
Deita	<u>75.17</u>	37.00	57.40	1/3	92.92%
COINCIDE	74.44	<u>40.40</u>	58.68	1/3	96.05%
mmSSR	<u>76.05</u>	<u>40.90</u>	<u>60.68</u>	3/3	<u>98.23%</u>
Budget: 30%					
Random	77.33	41.13	59.59	-	98.36%
Deita	76.88	40.00	59.56	0/3	97.24%
COINCIDE	<u>78.18</u>	41.00	<u>59.77</u>	2/3	<u>98.71%</u>
mmSSR	<u>78.13</u>	41.10	<u>59.80</u>	2/3	<u>98.78%</u>
FULL					
LLaVA-OVSI	79.27	41.40	60.70	-	100%

introduced in the pipeline. In this section, to verify the performance of the mmSSR judgments, we additionally annotated the remaining 85% of the single-image data pool with GPT-4o as a validation set. The mean absolute error (MAE) of the scorer is shown in Fig. 6(a). Overall, across 14 capabilities with varying levels of granularity and differentiation difficulty, an average of 77.7% of the scores are exactly the same as those given by GPT-4o. When allowing a margin of error of 1 in scoring, the accuracy reached 97.8%, which is a reasonable relaxation, considering that GPT’s pointwise judgment is not a definitive gold standard and may inherently contain fluctuations (Wettig et al., 2024).

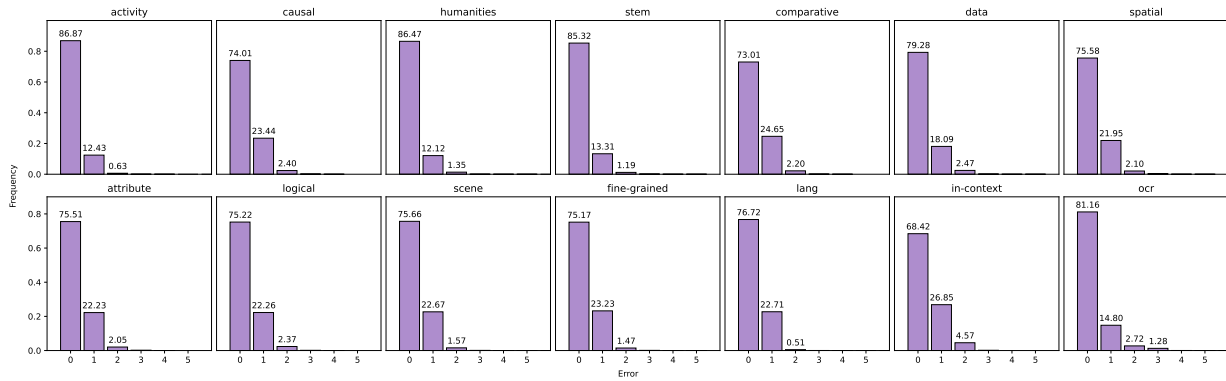
Based on the score distribution shown in Fig. 7, we observe that the accuracy of identifying rare and specialized abilities, such as those in the humanities and STEM fields, is relatively high, particularly in recognizing their absence. Consequently, in diversity-oriented sampling, such minority data are seldom overlooked. In contrast, while more ubiquitous abilities exhibit a normal or uniform distribution, giving completely identical scores is more challenging. In fact, if we randomly verify samples with closely related yet different scores, we observe that the differences in their values are often indistinguishable to human evaluators. For instance, in Fig. 21, the difference between scores of 1 and 2 in logical reasoning for the 4th example is minimal. Similarly, in Fig. 17, the distinction between values of 5 and 4 in comparative analysis for the 1st example is also minor.

We further increase the GPT-4o annotated data volume to 30% of the total dataset to train scorer. MAE results in Fig. 6(b) demonstrate a marginal performance improvement compared to models trained with 15% data, validating that the scoring models we derive has undergone sufficient training.

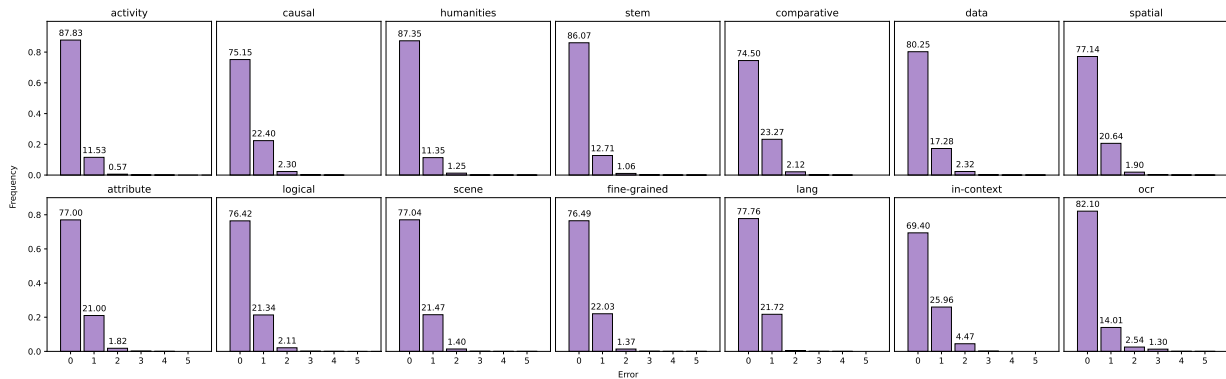
Thus, in summary, our mmSSR demonstrates the capability to deliver reliable and justified assessments when confronted with unseen multi-modal data.

C.2. Error Analysis of Styler

In Tab. 8, we present the precision and recall distributions of the styler against the GPT-4o recognition. Compared to the scoring task, determining the interaction style present in conversations is straightforward and yields higher accuracy. The



(a) mmSSR scorers trained with 15% data



(b) mmSSR scorers trained with 30% data

Figure 6. The mean absolute error of mmSSR scorer predictions against GPT-4o judgment over 14 capabilities.

average precision across the whole data pool reached 96.35%, while the recall achieved 95.80%.

C.3. Visualization of Capability Scores and Styler

For each capability of interest, we group the data based on GPT-4o’s scoring range of 0-5, randomly sample within each score group. Image-text pairs, GPT-4o scores, style recognition and explanations, and our mmSSR judgments are shown in Fig. 13-Fig. 26. The correspondence between capabilities and visualizations is detailed in Tab. 3.

D. Analysis of Selected Data

D.1. Scores of Selected Data

To illustrate the information obtained by our sampler, in Fig. 9, we present the score distributions of the selected subsets, focusing on two different sampling ratios: 10% and 30%. The scores used in the statistics are derived from the evaluations of our mmSSR trained with 15% scoring data. The distribution of total scores across all capabilities, as depicted in (a) and (c), manifests a bell-shaped curve. This characteristic shape is predominantly attributed to the limited availability of high-scoring options, which inherently restricts the sampler’s ability to select from the upper echelon of scores. Consequently, the distribution gravitates towards the central scores, forming a normal distribution pattern.

A notable aspect of our sampling approach is the selection of low scores despite their relatively modest total score contributions. Since selection is executed through a round-robin sampling methodology, which prioritizes minority yet specialized capabilities that have low synergy with other capabilities, such as STEM, which is critical for addressing niche challenges of benchmarks. The inclusion of these capabilities enhances the diversity and robustness of the sampled subset,

Cream of the Crop

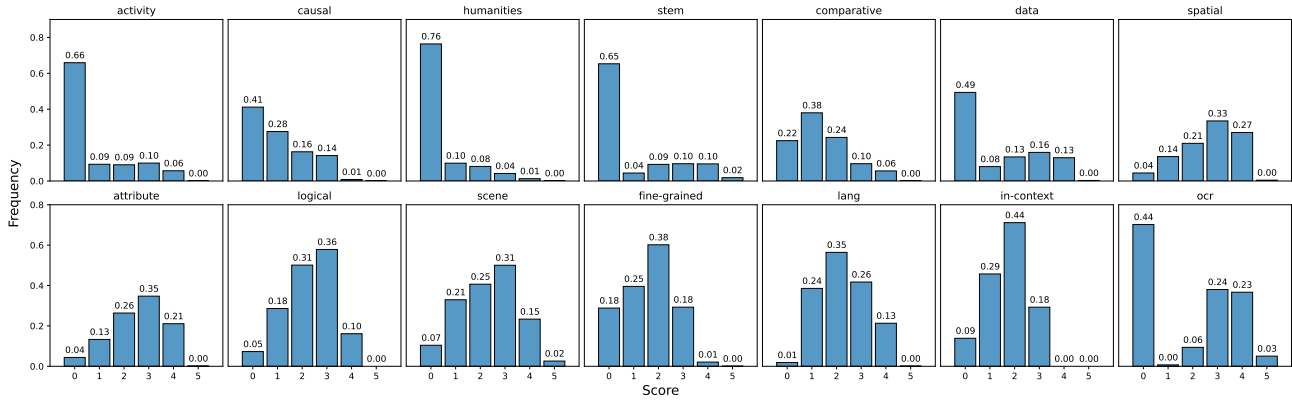
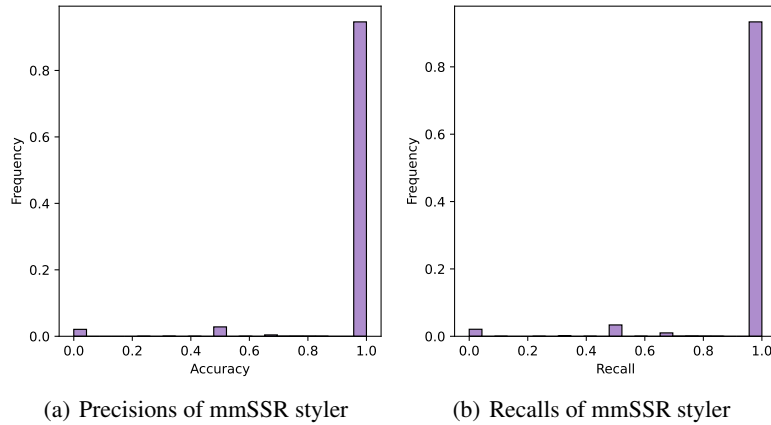


Figure 7. Distribution of scores on LLaVA-OVSI inferred by mmSSR.



(a) Precisions of mmSSR styler

(b) Recalls of mmSSR styler

Figure 8. The precision and recall of mmSSR styler predictions against GPT-4o judgment among 9 styles.

ensuring that our model is equipped to handle a broad spectrum of scenarios.

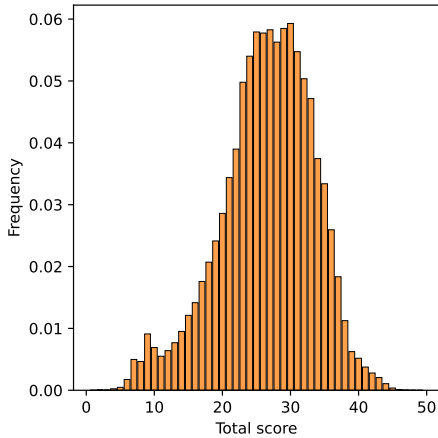
(b) and (d) further corroborate the sampler’s behavior, illustrating the distribution of maximum scores across all capabilities. The concentration of scores around the mid-range (specifically, scores of 4) underscores the mmSSR’s tendency to opt for samples with higher information efficiency.

By incorporating both highly-valued and specialized mid-range capabilities, our mmSSR not only ensures a balanced representation of capabilities but also reinforces the sampler’s capacity to enhance the overall performance and adaptability of the model.

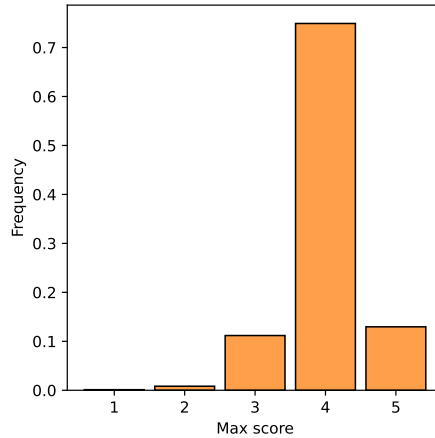
D.2. Sources of Selected Data

Considering the heterogeneity of multi-modal data sources and the challenges posed by extensive and comprehensive evaluation benchmarks, it is crucial to promote diversity in the instruction finetuning stage. Following the original data hierarchy (Li et al., 2024a), we detail the statistical information of the full data pool and our sampled 10% data in Tab. 5, and illustrate it in Fig. 10.

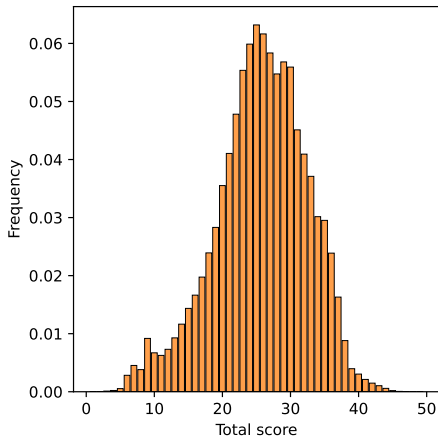
The subset reveal a shift towards balance when employing the proposed mmSSR. The original LLaVA-OVSI on the left, is dominated by the General category, which constitutes 42% of the data, in which COCO Caption makes up 35%. In contrast,



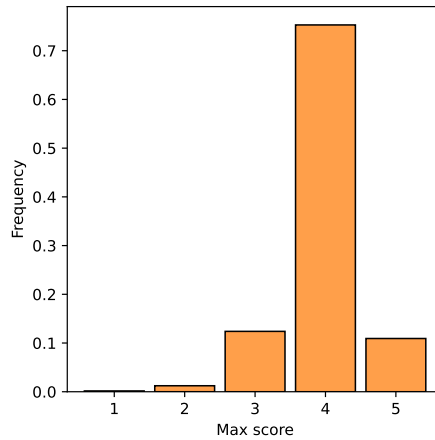
(a) Distribution of total scores across all capabilities for mmSSR-10%



(b) Distribution of the max score across all capabilities for mmSSR-10%



(c) Distribution of total scores across all capabilities for mmSSR-30%



(d) Distribution of the max score across all capabilities for mmSSR-30%

Figure 9. Score distribution analysis of the selected mmSSR-30%.

the subset on the right, sampled with mmSSR, shows a more balanced source distribution. Here, the General category is reduced to 35%, while COCO Caption decreases to 14%. Notably, the Math/Reasoning category expands from 24% to 29% in the sampled subset, and the Doc/Chart/Screen category increases from 26% to 31%. Fig. 11 highlights the differences between comparative methods and ours. Notably, mmSSR exhibits a more balanced distribution across various sources, while Deita and E5-V embedding shows a pronounced concentration in the dominant general data, PPL and CLIP favor math/reasoning data, especially Visual Genome, over others, and COINCIDE is skewed towards Doc/Chart/Screen. The effective reallocation of training data underscore the advantages of mmSSR in achieving a more equitable representation of data sources, enhancing the robustness of the fine-tuned model in general instruction-following tasks and improving its adaptability for more challenging tasks, such as mathematical problem-solving and infographic reasoning.

D.3. Styles of Selected Data

Likewise, we provide a comparative analysis of the data style distributions in Fig. 12. As can be seen, our mmSSR exhibits a distinct distribution pattern characterized by a balanced representation of several key styles. This distribution indicates a comprehensive and balanced coverage of styles that are essential for the SFT stage, thereby enhancing the robustness of the finetuned model. In comparison, other sampling methods show a skewed distribution, with certain styles, like *detailed description* that usually contributes more training tokens, and *yes/no* or *word/short-phrase* that is ubiquitous in benchmarks,

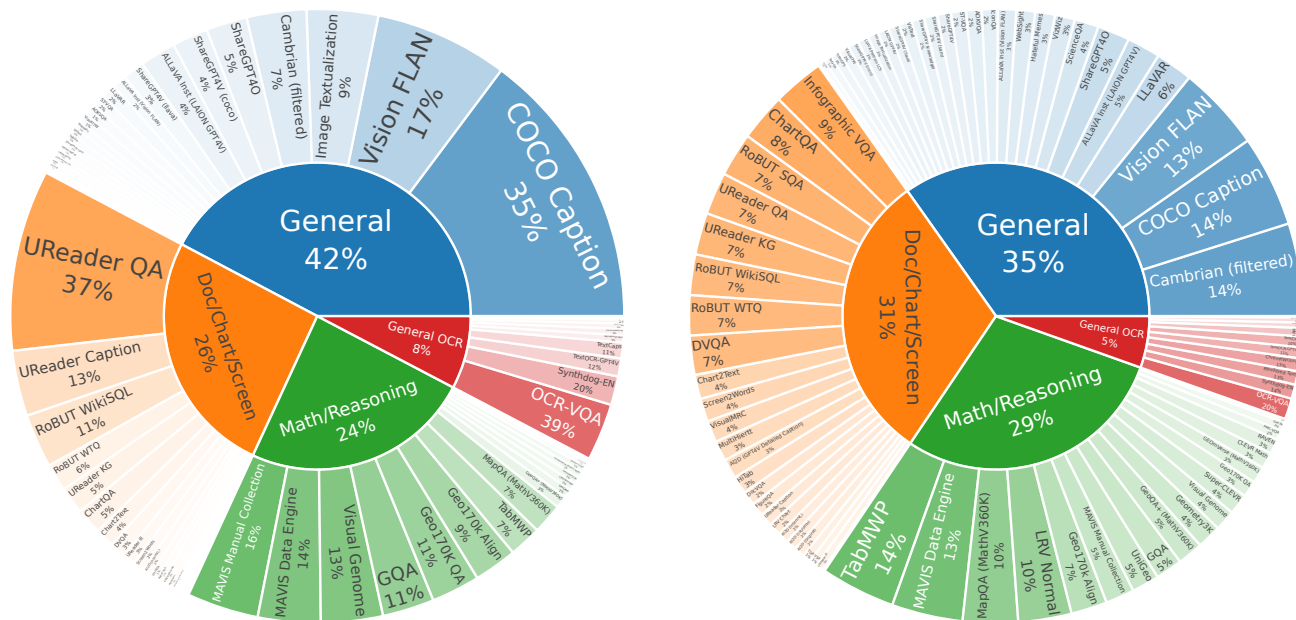


Figure 10. Data source statistics of the original LLaVA-OVSI data pool (L) and our mmSSR-10% (R).

being overrepresented. The imbalance could potentially limit the versatility and applicability of the datasets generated by these methods. Notably, our approach achieves a more equitable distribution across different styles, including *comparison* and *chain-of-thought*, which are crucial for reasoning tasks. This balanced distribution is indicative of our method’s capability to cater to a broader range of machine learning applications, thereby positioning our sampling method as a versatile tool for dataset curation.

In summary, the analysis in Fig. 9, 10, 11 and 12 demonstrates that mmSSR can provide a highly informative subset over rich capabilities, which enjoying a well-rounded and diverse dataset composition over both data sources and instruction styles, contributing to the data efficiency and explainability of MLLMs.

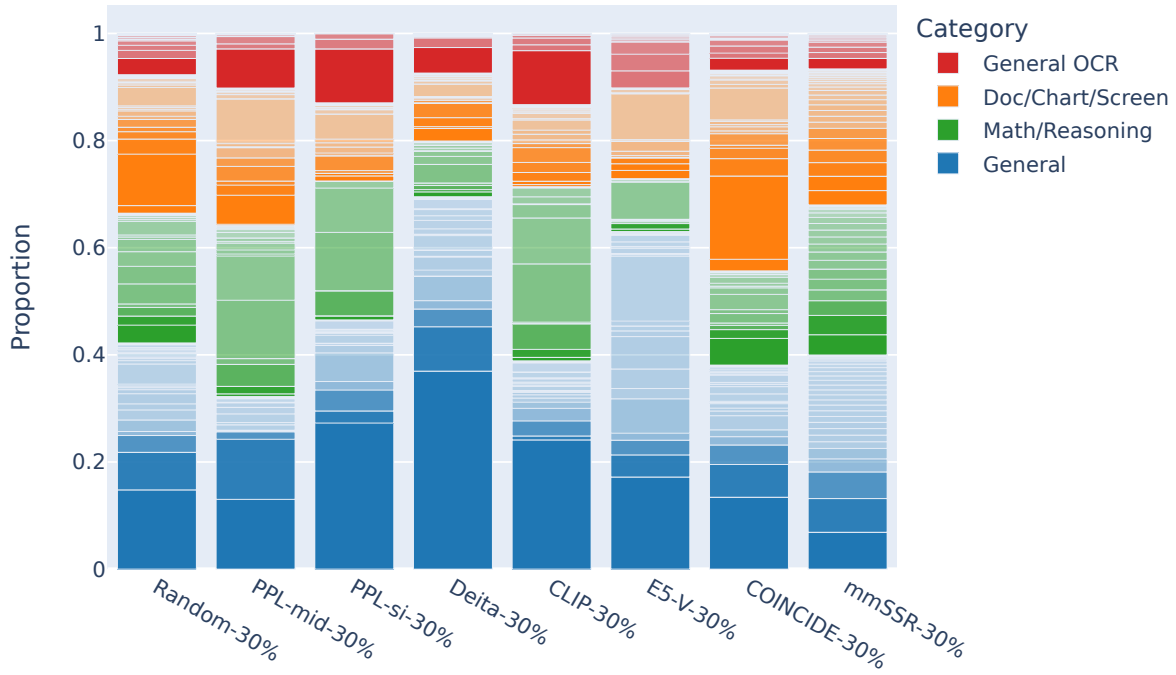


Figure 11. Comparison of data source statistics between our selection and those of competitors. For brevity, the figure displays only a small subset of the legends. Data sources of the same category are represented by shared color schemes, in accordance with Fig. 10.

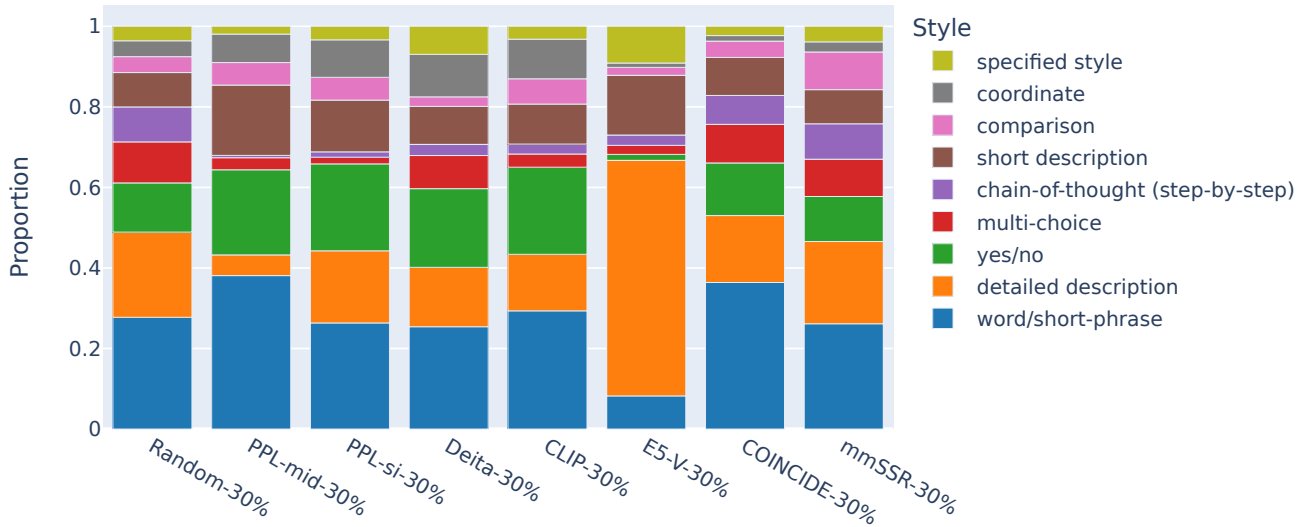


Figure 12. Comparison of data style statistics between our selection and those of competitors.

Cream of the Crop

Table 5: Counts and Ratios of Subclasses for Each DataFrame

Source	LLaVA-OVSI		mmSSR-10%		mmSSR-30%	
	# Samples	Proportion	# Samples	Proportion	# Samples	Proportion
General						
COCO Caption	391219	34.97%	12828	13.83%	54707	17.21%
Vision FLAN	186060	16.63%	11922	12.85%	50068	15.75%
Image Textualization	99573	8.90%	1523	1.64%	7760	2.44%
Cambrian (filtered)	83125	7.43%	12997	14.01%	39517	12.43%
ShareGPT4O	57284	5.12%	4533	4.89%	15400	4.84%
ShareGPT4V (coco)	50017	4.47%	1510	1.63%	9755	3.07%
ALLaVA Inst (LAION GPT4V)	49990	4.47%	4696	5.06%	9976	3.14%
ShareGPT4V (llava)	29990	2.68%	1613	1.74%	9768	3.07%
ALLaVA Inst (Vision FLAN)	19990	1.79%	2577	2.78%	9220	2.90%
LLaVAR	19790	1.77%	5231	5.64%	19509	6.14%
ST-VQA	17242	1.54%	2096	2.26%	7013	2.21%
AOKVQA	16534	1.48%	2188	2.36%	7486	2.35%
Visual7W	14361	1.28%	1478	1.59%	4802	1.51%
WebSight	9995	0.89%	2632	2.84%	8742	2.75%
VisText	9964	0.89%	1769	1.91%	6363	2.00%
TallyQA	9868	0.88%	1126	1.21%	7309	2.30%
ShareGPT4V (sam)	8990	0.80%	1862	2.01%	8451	2.66%
Hateful Memes	8495	0.76%	2765	2.98%	8495	2.67%
LAION GPT4V	8048	0.72%	1525	1.64%	7139	2.25%
LLaVA Pretrain LCS	6989	0.62%	1512	1.63%	6580	2.07%
VizWiz	6604	0.59%	2809	3.03%	5220	1.64%
ScienceQA	5932	0.53%	3388	3.65%	5930	1.87%
IconQA	2496	0.22%	2214	2.39%	2496	0.79%
ShareGPT4V (knowledge)	1988	0.18%	1770	1.91%	1988	0.63%
ShareGPT4V	1926	0.17%	1911	2.06%	1926	0.61%
InterGPS	1275	0.11%	1275	1.37%	1275	0.40%
CLEVR	700	0.06%	700	0.75%	700	0.22%
VQARAD	308	0.03%	308	0.33%	308	0.10%
Doc/Chart/Screen						
UReader QA	252954	36.96%	5962	7.27%	21233	10.51%
UReader Caption	91434	13.36%	1784	2.18%	6861	3.40%
RoBUT WikiSQL	74984	10.95%	5688	6.94%	20290	10.05%
RoBUT WTQ	38241	5.59%	5622	6.86%	15094	7.47%
UReader KG	37550	5.49%	5872	7.16%	21335	10.56%
ChartQA	36577	5.34%	6669	8.14%	18550	9.18%
Chart2Text	26956	3.94%	3403	4.15%	8751	4.33%
DVQA	22000	3.21%	5489	6.70%	17219	8.52%
UReader IE	17322	2.53%	1060	1.29%	3307	1.64%
Screen2Words	15725	2.30%	3256	3.97%	9225	4.57%
AI2D (InternVL)	12403	1.81%	1530	1.87%	6715	3.32%
DocVQA	10194	1.49%	1999	2.44%	5272	2.61%
RoBUT SQA	8509	1.24%	6148	7.50%	8509	4.21%
Infographic VQA	8489	1.24%	7233	8.82%	8489	4.20%
MultiHiertt	7614	1.11%	2855	3.48%	7614	3.77%

Continued on next page

Cream of the Crop

Source	LLaVA-OVSI		mmSSR-10%		mmSSR-30%	
	# Samples	Proportion	# Samples	Proportion	# Samples	Proportion
AI2D (GPT4V Detailed Caption)	4864	0.71%	2746	3.35%	4864	2.41%
AI2D (Original)	3247	0.47%	1457	1.78%	3247	1.61%
VisualMRC	3022	0.44%	3021	3.69%	3022	1.50%
HiTab	2495	0.36%	2495	3.04%	2495	1.24%
AI2D (cauldron)	2429	0.35%	1499	1.83%	2429	1.20%
VSR	2152	0.31%	1062	1.30%	2152	1.07%
FigureQA	1880	0.27%	1880	2.29%	1880	0.93%
LRV Chart	1776	0.26%	1776	2.17%	1776	0.88%
TQA	1366	0.20%	1177	1.44%	1366	0.68%
Diagram Image2Text	295	0.04%	295	0.36%	295	0.15%
Math/Reasoning						
MAVIS Manual Collection	99990	15.60%	4033	5.22%	15763	7.08%
MAVIS Data Engine	87348	13.63%	9964	12.90%	30124	13.52%
Visual Genome	86417	13.49%	2895	3.75%	14992	6.73%
GQA	72140	11.26%	3771	4.88%	13056	5.86%
Geo170K QA	67823	10.58%	2330	3.02%	10150	4.56%
Geo170k Align	60242	9.40%	5067	6.56%	12398	5.56%
TabMWP	45169	7.05%	10516	13.61%	28677	12.87%
MapQA (MathV360K)	42637	6.65%	7735	10.01%	21827	9.80%
GeoQA+ (MathV360K)	17162	2.68%	3578	4.63%	16106	7.23%
UniGeo	11949	1.86%	3855	4.99%	11947	5.36%
LRV Normal	10489	1.64%	7481	9.68%	10489	4.71%
Geometry3K	9724	1.52%	3415	4.42%	9724	4.36%
GEOmVerse (MathV360K)	9298	1.45%	2326	3.01%	9029	4.05%
Super-CLEVR	8642	1.35%	2883	3.73%	6774	3.04%
CLEVR Math	5280	0.82%	2248	2.91%	5248	2.36%
RAVEN	2100	0.33%	2100	2.72%	2100	0.94%
Geo3k	2091	0.33%	1165	1.51%	2091	0.94%
PMC-VQA	1798	0.28%	1387	1.80%	1797	0.81%
GEOS	498	0.08%	498	0.64%	498	0.22%
General OCR						
OCR-VQA	80000	39.29%	2942	20.29%	15556	29.56%
Synthdog-EN	40093	19.69%	2006	13.84%	8730	16.59%
TextOCR-GPT4V	25104	12.33%	1528	10.54%	8013	15.23%
TextCaps	21942	10.78%	1520	10.48%	7262	13.80%
Rendered Text	9995	4.91%	1881	12.97%	2796	5.31%
ChromeWriting	8825	4.33%	1813	12.50%	3277	6.23%
HME100K	7450	3.66%	761	5.25%	3364	6.39%
IAM	5658	2.78%	1167	8.05%	2151	4.09%
K12 Printing	2567	1.26%	710	4.90%	982	1.87%
IIIT5K	1990	0.98%	171	1.18%	486	0.92%



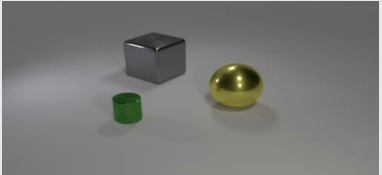



spatial	Image	QA Pairs	mmSSR
<p>GPT4o</p> <p>Score: 5</p> <p>Style: coordinate</p>	 <p>Explanation: The task requires identifying precise locations of objects, enhancing spatial understanding.</p>	<p>Q: Provide the bounding box coordinates of the region that the given sentence describes. The passing vehicle.</p> <p>A: [0.000,0.000,0.662,0.757]</p> <p>Q: A large black and dark green backpack on the ground.</p> <p>A: [0.253,0.465,0.500,0.991]</p> <p>Q: The bus that is behind the luggage and the person on the sidewalk. it is in motion.</p> <p>A: [0.000,0.000,0.662,0.757]</p> <p>...</p>	<p>Score: 5</p> <p>Style: coordinate</p>
<p>Score: 4</p> <p>Style: multi-choice, yes/no</p>	 <p>Explanation: The image requires understanding of symmetry and spatial alignment.</p>	<p>Q: Is the dotted line a line of symmetry? Choices: A. yes B. no Answer with the option's letter from the given choices directly.</p> <p>A: A</p> <p>Q: Does this picture have symmetry? Choices: A. no B. yes Answer with the option's letter from the given choices directly.</p> <p>A: B</p>	<p>Score: 4</p> <p>Style: multi-choice, yes/no</p>
<p>Score: 3</p> <p>Style: detailed description</p>	 <p>Explanation: The description includes spatial relationships, aiding understanding.</p>	<p>Q: Can you describe the lighting in the scene?</p> <p>A: The lighting in the scene appears to be diffused, with a soft shadow cast beneath each object, indicating an overhead light source that is not too harsh. There are no strong highlights, which suggests the lighting is even and possibly from a studio light setup or image rendering with a global illumination feature for realistic lighting.</p>	<p>Score: 3</p> <p>Style: detailed description</p>
<p>Score: 2</p> <p>Style: detailed description</p>	 <p>Explanation: Some spatial understanding is possible, but the description is inaccurate.</p>	<p>Q: What's happening in the scene?</p> <p>A: The image features a white plate holding a delicious meal, consisting of a half-eaten sandwich on a roll, which occupies most of the space, and a side salad placed near the front left corner of the plate. The salad is made up of various mixed vegetables such as broccoli, cauliflower, cabbage, and other greens. In the front of the plate, closer to the camera, a glazed tan round donut hole is positioned. The arrangement creates a visually appealing and appetizing dish.</p>	<p>Score: 2</p> <p>Style: detailed description</p>
<p>Score: 1</p> <p>Style: yes/no, word/short-phrase</p>	 <p>Explanation: No spatial relationship with a dark car is visible.</p>	<p>Q: Is the hydrant to the left or to the right of the dark car? Answer the question using a single word or phrase.</p> <p>A: Left</p> <p>Q: What is common to the sign and the fire hydrant?</p> <p>A: Color</p> <p>Q: Which place is it?</p> <p>A: Road</p> <p>Q: Is there any black signal light or fire hydrant?</p> <p>A: No</p>	<p>Score: 4</p> <p>Style: yes/no, word/short-phrase</p>
<p>Score: 0</p> <p>Style: detailed description</p>	 <p>Explanation: No spatial relationships or object positions are relevant in this context.</p>	<p>Q: Considering the specific project title listed under "CURRENT FUNDING OPPORTUNITIES", what could be the focus of research for Early Stage Researchers in the context of "Tendon Repair, Network of Excellence for Functional Biomaterials"?</p> <p>A: Based on the project title, the focus of research for Early Stage Researchers is likely to be on developing or improving biomaterials that can be used in the repair of tendons. The "Network of Excellence" suggests a collaborative effort, potentially involving multiple institutions or departments, aimed at innovating in the field of functional biomaterials specifically for tendon repair applications.</p>	<p>Score: 0</p> <p>Style: detailed description</p>

Figure 13. Randomly selected samples from the LLaVA-OVSI data pool within each score group for the activity recognition capability, ranging from 5 to 0, as evaluated by GPT-4, along with corresponding score explanations and mmSSR predictions.





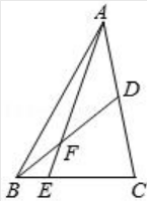

attribute	Image	QA Pairs	mmSSR
GPT4o		<p>Q: Can you describe all the objects and characters in the picture?</p> <p>A: The image depicts a wristwatch with a prominent and detail-rich dial, set against a green backdrop. To the right bottom corner, a part of a date-stamped paper is visible. The watch is contained in a transparent plastic protective case or wrapper. Here is a detailed description and analysis: ### Watch Dial: - **Brand and Model**: The brand name "Audemars Piguet" can be read on the dial, indicating this is a luxury timepiece highly regarded in ...</p>	<p>Score: 5</p> <p>Style: detailed description, chain-of-thought</p>
Score: 5	<i>Explanation: Detailed attributes of the watch are identified, including brand, color, and features.</i>		
Score: 4		<p>Q: Why are the cows wearing ribbons? Answer the question using a single word or phrase.</p> <p>A: 1</p> <p>Q: Is the man wearing a hat?</p> <p>A: Yes</p> <p>Q: What number is on the cow?</p> <p>A: 3010</p> <p>Q: How many different types of head coverings are people wearing?</p> <p>A: 1</p> <p>Q: Does this cow have black and white spots?</p> <p>A: Yes</p> <p>Q: How tall is the cow?</p> <p>...</p>	<p>Score: 4</p> <p>Style: multi-choice, yes/no</p>
Score: 4	<i>Explanation: Attributes like the cow's color and the man's hat are correctly identified.</i>		
Score: 3		<p>Q: Render a clear and concise summary of the photo.</p> <p>A: Procomm Plus written in blue on a computer</p>	<p>Score: 3</p> <p>Style: short description</p>
Score: 3	<i>Explanation: Identifying the computer and its screen provides moderate attribute information.</i>		
Score: 2		<p>Q: they lose the first game to the new orleans saint the final score be 31 - 24, Yes or No? Answer the question using a single word or phrase.</p> <p>A: Yes</p>	<p>Score: 2</p> <p>Style: yes/no, word/short phrase</p>
Score: 2	<i>Explanation: Some identification of game results is needed, but it's minimal.</i>		
Score: 1		<p>Q: Describe what you see in the figure.</p> <p>A: In the diagram, there is a triangle labeled ABC, with points A, B, and C as its vertices. On the line segment BC, there's a point named E. Point D is the midpoint of the line segment AC.</p>	<p>Score: 2</p> <p>Style: detailed description</p>
Score: 1	<i>Explanation: Minimal attributes are identified in the description.</i>		
Score: 0		<p>Q: What might be the implications of the viewpoint expressed in the tweet regarding the use of encryption in consumer products, and how could this stance affect the privacy and security landscape if implemented as a policy?</p> <p>A: Based on the tweet, the user is expressing a stance against the use of encryption for routine communications in consumer products, suggesting that security should be ...</p>	<p>Score: 0</p> <p>Style: detailed description</p>
Score: 0	<i>Explanation: No attributes of objects are identified in this instance.</i>		

Figure 14. Randomly selected samples from the LLaVA-OVSI data pool within each score group for the **causal reasoning** capability, ranging from 5 to 0, as evaluated by GPT-4, along with corresponding score explanations and mmSSR predictions.

logical	Image	QA Pairs	mmSSR
GPT4o		<p>Q: Which figure should complete the logical sequence?</p> <p>A: G</p>	<p>Score: 5</p> <p>Style: multi-choice</p>
Score: 4		<p>Q: According to the question shown in the image, please first conduct reasoning, and then answer the question and provide the final value, e.g., The answer is xxx Question: Based on the image, what is the shape of the region D where the double integration is performed?</p> <p>A: Region D where the double integration takes place is shown as a circular disk in the yz-plane. The limits for this region are derived from the intersection of the paraboloid and the plane, yielding a circle of radius $\sqrt{3}$, which is highlighted in the diagram. So the answer is circular disk.</p>	<p>Score: 4</p> <p>Style: word/sh ort-phrase, chain-of-thought</p>
Score: 3		<p>Q: What time of day and season could this painting be representing based on the lighting and the activities of the people?</p> <p>A: The painting could be representing late morning to early afternoon, as the light is bright but diffused, suggesting the sun is not at its peak. The presence of clouds might be blocking the direct sunlight, casting a soft glow over the landscape. The season appears to be either late spring or early autumn, as the fields are lush but not in the height of summer growth, ...</p>	<p>Score: 3</p> <p>Style: detailed description</p>
Score: 2		<p>Q: You are provided with a picture, write a caption with a specific sentiment (positive or negative) related to the picture. Note that the sentiment in the caption should match the requested sentiment. Write a caption with a negative sentiment for the given image.</p> <p>A: a horrible picture of people at the mountain ski resort</p>	<p>Score: 1</p> <p>Style: specified style</p>
Score: 1		<p>Q: What was the value share of Scotch whisky in the United States in 2014? Answer the question using a single word or phrase.</p> <p>A: 750.</p>	<p>Score: 3</p> <p>Style: word/sh ort-phrase</p>
Score: 0		<p>Q: Here is a picture of a person. Based only upon this picture, what would you guess this person's gender is?</p> <p>A: The person's gender is Male</p>	<p>Score: 0</p> <p>Style: word/sh ort-phrase</p>

Figure 15. Randomly selected samples from the LLaVA-OVSI data pool within each score group for the **humanities** capability, ranging from 5 to 0, as evaluated by GPT-4, along with corresponding score explanations and mmSSR predictions.


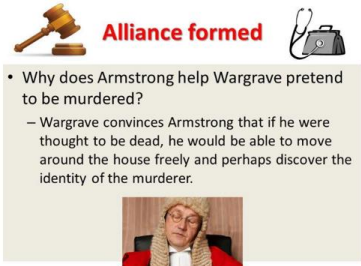

scene	Image	QA Pairs	mmSSR
GPT4o		<p>Q: Describe this image in detail.</p> <p>A: The image captures the entrance to the City Museum in St. Louis, Missouri. Dominating the scene is a large, rusted metal gate that serves as the main entrance. The gate is adorned with a sign that spells out "City Museum" in vibrant, colorful letters. On either side of the gate, two imposing metal sculptures stand guard. One of these sculptures takes the form of a dragon, adding a touch of whimsy to the scene. The ground beneath these structures is blanketed with fallen leaves, hinting at a season change...</p>	<p>Score: 5</p> <p>Style: detailed description</p>
Score: 5		<p>Q: Describe this image in detail.</p> <p>A: In the midst of a snowy landscape, a pair of legs clad in vibrant orange ski boots stand confidently. The boots, adorned with black buckles, are firmly attached to a pair of brown skis streaked with white stripes. The skis cut a striking contrast against the pristine white snow, which appears freshly fallen and untouched except for a few tracks in the background. In the skier's grip are two ski poles, their black shafts ending in white handles. The poles are poised as if ready to push off into the snow at any moment...</p>	<p>Score: 4</p> <p>Style: detailed description</p>
Score: 4		<p>Q: Considering the context provided in the slide, what could be the significance of the symbols of the gavel and medical bag in relation to the text presented?</p> <p>A: The gavel and the medical bag symbols next to the title "Alliance formed" suggest that the alliance involves legal and medical aspects. This is supported by the text, which refers to characters named Armstrong and Wargrave. Armstrong is likely a medical professional, suggested by the medical bag, and Wargrave, who may be the person in the judge's robe, represents the legal side, indicated by the gavel. These symbols are visual cues to the professions or roles of the characters involved ...</p>	<p>Score: 3</p> <p>Style: detailed description</p>
Score: 3		<p>Q: What are the initials on the train? Answer the question using a single word or phrase.</p> <p>A: BNSF.</p>	<p>Score: 2</p> <p>Style: word/short-phrase</p>
Score: 2		<p>Q: Look at the table. Then answer the question. At a price of \$710, is there a shortage or a surplus?</p> <p>A: At the price of \$710, the quantity demanded is greater than the quantity supplied. There is not enough of the good or service for sale at that price. So, there is a shortage.</p>	<p>Score: 1</p> <p>Style: detailed description</p>
Score: 1		<p>Q: What's written in this image?</p> <p>A: A flying saucer was tilting and dipping over the War Memorial.</p>	<p>Score: 0</p> <p>Style: word/short-phrase</p>
Score: 0			

Figure 16. Randomly selected samples from the LLaVA-OVSI data pool within each score group for the **stem knowledge** capability, ranging from 5 to 0, as evaluated by GPT-4, along with corresponding score explanations and mmSSR predictions.





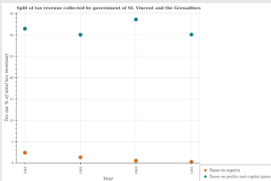

fine-grained	Image	QA Pairs	mmSSR
<p>GPT4o</p> <p>Score: 5</p> <p>Style: word/short-phrase</p>	 <p>Explanation: High level of detail needed to distinguish aircraft variant.</p>	<p>Q: Your objective is to analyze an aircraft image and provide the variant of the aircraft. (e.g., A300B4). Variant: A variant indicates a variation of a particular aircraft model, often incorporating specific modifications, improvements, or customizations compared to the base model. A: BAE 146-300</p>	<p>Score: 5</p> <p>Style: word/short-phrase</p>
<p>Score: 4</p> <p>Style: detailed description</p>	 <p>Explanation: Specific brain structures are identified with some detail.</p>	<p>Q: Describe the content of a given image in detail A: This image is an MRI scan of a human brain, oriented to provide an axial view. An MRI (Magnetic Resonance Imaging) scan uses strong magnetic fields and radio waves to generate detailed images of the inside of the body, particularly the soft tissues. In this particular slice, we can observe several key structures of the brain. 1. Cerebral Hemispheres: The left and right cerebral hemispheres are clearly visible. The presence of sulci and gyri, the folds of the brain, is evident although not extremely detailed in this specific slice. 2. Corpus Callosum: The corpus callosum...</p>	<p>Score: 4</p> <p>Style: detailed description</p>
<p>Score: 3</p> <p>Style: multi-choice</p>	 <p>Explanation: Recognizing specific features of the elephant is required.</p>	<p>Q: Considering the size of his ears what continent is this elephant from? A. north america B. asia C. africa D. europe Answer with the option's letter from the given choices directly. A: B</p>	<p>Score: 3</p> <p>Style: multi-choice</p>
<p>Score: 2</p> <p>Style: word/short-phrase, yes/no</p>	 <p>Explanation: Limited detail on the plane's specific model or era.</p>	<p>Q: What continent is this plane flying over? Answer the question using a single word or phrase. A: Antarctica Q: What is below the plane? A: Mountains Q: Is this a plane made after the year 2000? A: No</p>	<p>Score: 2</p> <p>Style: word/short-phrase, yes/no</p>
<p>Score: 1</p> <p>Style: comparison</p>	 <p>Explanation: Minimal need for distinguishing subtle differences.</p>	<p>Q: You are provided with a chart image and a question related to the chart. Answer the question based on the information given in the chart. In the year 1992, what is the difference between the percentage of revenue obtained from taxes on profits and capital gains and percentage of revenue obtained from taxes on exports ? A: 29.05551550108148</p>	<p>Score: 1</p> <p>Style: comparison</p>
<p>Score: 0</p> <p>Style: multi-choice, chain-of-thought</p>	 <p>Explanation: No fine-grained recognition is needed for the image.</p>	<p>Q: According to the question shown in the image, please first perform reasoning, then finally select the right answer from the choices, e.g., Answer: xxx. Question: Based on the image, what mathematical operation is used on side \$b\$ and the hypotenuse to find side \$a\$? Choices: A. Addition B. Subtraction C. Multiplication D. Division A: You square and then subtract the measurements to solve for side \$a\$ using the Pythagorean theorem. So the answer is B Answer: B</p>	<p>Score: 0</p> <p>Style: multi-choice, chain-of-thought</p>

Figure 17. Randomly selected samples from the LLaVA-OVSI data pool within each score group for the **comparative analysis** capability, ranging from 5 to 0, as evaluated by GPT-4, along with corresponding score explanations and mmSSR predictions.




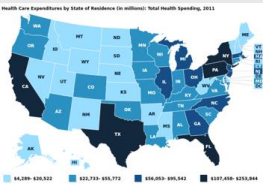
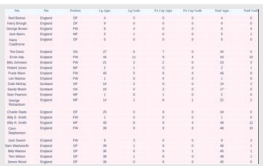

lang	Image	QA Pairs	mmSSR
GPT4o		<p>Q: Analyze and describe in detail the visual elements in this image.</p> <p>A: The image showcases a vibrant town square that includes a well-preserved, large stone column monument at its center. This column appears to be an artistic sculpture featuring multiple figures and intricate carvings. The column is the central focus and reaches a significant height, visually dominating the scene. Atop the column, there is a prominent figure holding a cross, which is accented in gold, suggesting religious significance. Surrounding this central figure are several other figures, possibly angels or historical characters, integrated into the structure with dynamic, flowing poses. The immediate surroundings are ...</p>	<p>Score: 5</p> <p>Style: detailed description</p>
	<i>Explanation: The answer is well-structured and detailed, showcasing strong language generation.</i>		
		<p>Q: What do you see happening in this image?</p> <p>A: The image captures a moment at a train station. On the left, a vibrant yellow and blue train, with a yellow front, is approaching the viewer from a distance, moving towards the camera on the right track, as if ready to embark on a new journey. On the right side of the image, close to the camera, another train is seen. This one is adorned in red and white, with a moving away from the viewer on the left track, as if it has completed its journey and is now returning. The station itself, with its red roof, nestles comfortably in the background. It's a silent observer to the comings and goings of these mechanical beasts ...</p>	<p>Score: 4</p> <p>Style: detailed description</p>
	<i>Explanation: The answer is well-articulated and descriptive.</i>		
		<p>Q: Provide a one-sentence caption for the provided image.</p> <p>A: The clock shows one hand at around 10 and another at around 12.</p>	<p>Score: 2</p> <p>Style: short description</p>
	<i>Explanation: The task involves generating a coherent caption.</i>		
		<p>Q: What is the value of Idaho? Answer the question using a single word or phrase.</p> <p>A: 4,289-20,522.</p> <p>Q: Name the states that have a value in the range 107,458-253,844?</p> <p>A: California, Florida, New York, Pennsylvania, Texas. ...</p>	<p>Score: 2</p> <p>Style: word/short phrase, yes/no, comparison</p>
	<i>Explanation: Limited generation of responses based on map data.</i>		
		<p>Q: What are the number of league apps ted davis has? Answer the question using a single word or phrase.</p> <p>A: 27.</p>	<p>Score: 1</p> <p>Style: word/short phrase</p>
	<i>Explanation: Minimal language generation required.</i>		
		<p>Q: Provide the bounding box coordinates of the region that the given sentence describes. Hitter.</p> <p>A: [0.491,0.281,0.720,0.771]</p> <p>Q: Catcher.</p> <p>A: [0.122,0.496,0.380,0.796]</p> <p>...</p>	<p>Score: 0</p> <p>Style: coordinate</p>
	<i>Explanation: No language generation required.</i>		

Figure 18. Randomly selected samples from the LLaVA-OVSI data pool within each score group for the **data understanding** capability, ranging from 5 to 0, as evaluated by GPT-4, along with corresponding score explanations and mmSSR predictions.

in-context	Image	QA Pairs	mmSSR																																																																	
GPT4o Score: 5 Style: detailed description, short description	 <p>Explanation: The instance follows the task instructions and provides answers in the specified format.'</p>	Q: What are the main features of the kitchen in the image? Answer the question with GPT-T-COCO format. A: The main features of the kitchen in the image include a stove with an oven, a table, various pots and utensils, and a light that is turned on next to the stove. The kitchen has a rustic appearance. Q: Is there anything placed on top of the oven? A: Yes, there is a bowl placed on top of the oven. Q: What is the overall size of the kitchen? ...	Score: 3 Style: detailed description, short description																																																																	
Score: 4 Style: detailed description, specified style	 <p>Explanation: The speculative scenario provides a creative context for learning.</p>	Q: Explain the significance of the main character's attire. A: The main character's attire is highly significant, as it reflects the fashion and societal norms of a specific historical period. Dressed in a black suit with a formal shirt and a meticulously groomed beard, he presents a dignified and authoritative figure. Such attire was typical for gentlemen in the 19th century, particularly those in positions of power or influence, such as lawyers, politicians, or other public figures. This choice of clothing helps to convey the character's social status and the serious nature of the proceedings he is involved in. Q: What does the presence of the American flags behind him symbolize? ...	Score: 3 Style: detailed description, specified style																																																																	
Score: 3 Style: multi-choice	 <p>Explanation: Follows the task format and context well.</p>	Q: What type of animal is featured in the image alongside the babies? Answer the question with GPT-T-COCO format. A: The image features a mother sheep, also known as a ewe, alongside her two baby sheep, also known as lambs. Q: What are the baby lambs doing in the image? A: In the image, one baby lamb is eating from its mother, while the other baby lamb is eating grass. ...	Score: 3 Style: multi-choice																																																																	
Score: 2 Style: word/short phrase, yes/no	<table border="1"> <thead> <tr> <th>Place</th> <th>Player</th> <th>Country</th> <th>Score</th> <th>To par</th> </tr> </thead> <tbody> <tr> <td>1</td> <td>Bobby Clampett</td> <td>United States</td> <td>67-66=133</td> <td>-11</td> </tr> <tr> <td>2</td> <td>Nick Price</td> <td>Zimbabwe</td> <td>69-69=138</td> <td>-6</td> </tr> <tr> <td>T2</td> <td>Bernhard Langer</td> <td>West Germany</td> <td>70-69=139</td> <td>-5</td> </tr> <tr> <td></td> <td>Des Smyth</td> <td>Ireland</td> <td>70-69=139</td> <td>-5</td> </tr> <tr> <td>T5</td> <td>Sandy Lyle</td> <td>Scotland</td> <td>74-66=140</td> <td>-4</td> </tr> <tr> <td></td> <td>Tom Watson</td> <td>United States</td> <td>69-71=140</td> <td>-4</td> </tr> <tr> <td>T7</td> <td>Kan Brown</td> <td>Scotland</td> <td>70=71=141</td> <td>-3</td> </tr> <tr> <td></td> <td>Peter Oosterhuis</td> <td>England</td> <td>74-67=141</td> <td>-3</td> </tr> <tr> <td>9</td> <td>Tom Purtzer</td> <td>United States</td> <td>76-66=142</td> <td>-2</td> </tr> <tr> <td></td> <td>José María Cañizares</td> <td>Spain</td> <td>71-72=143</td> <td>-1</td> </tr> <tr> <td>T10</td> <td>David Graham</td> <td>Australia</td> <td>73-70=143</td> <td>-1</td> </tr> <tr> <td></td> <td>Bill Rogers</td> <td>United States</td> <td>73-70=143</td> <td>-1</td> </tr> </tbody> </table> <p>Explanation: Limited demonstration of task understanding.</p>	Place	Player	Country	Score	To par	1	Bobby Clampett	United States	67-66=133	-11	2	Nick Price	Zimbabwe	69-69=138	-6	T2	Bernhard Langer	West Germany	70-69=139	-5		Des Smyth	Ireland	70-69=139	-5	T5	Sandy Lyle	Scotland	74-66=140	-4		Tom Watson	United States	69-71=140	-4	T7	Kan Brown	Scotland	70=71=141	-3		Peter Oosterhuis	England	74-67=141	-3	9	Tom Purtzer	United States	76-66=142	-2		José María Cañizares	Spain	71-72=143	-1	T10	David Graham	Australia	73-70=143	-1		Bill Rogers	United States	73-70=143	-1	Q: 2 athlete finish 4 below par, Yes or No? Answer the question using a single word or phrase. A: Yes	Score: 2 Style: word/short phrase, yes/no
Place	Player	Country	Score	To par																																																																
1	Bobby Clampett	United States	67-66=133	-11																																																																
2	Nick Price	Zimbabwe	69-69=138	-6																																																																
T2	Bernhard Langer	West Germany	70-69=139	-5																																																																
	Des Smyth	Ireland	70-69=139	-5																																																																
T5	Sandy Lyle	Scotland	74-66=140	-4																																																																
	Tom Watson	United States	69-71=140	-4																																																																
T7	Kan Brown	Scotland	70=71=141	-3																																																																
	Peter Oosterhuis	England	74-67=141	-3																																																																
9	Tom Purtzer	United States	76-66=142	-2																																																																
	José María Cañizares	Spain	71-72=143	-1																																																																
T10	David Graham	Australia	73-70=143	-1																																																																
	Bill Rogers	United States	73-70=143	-1																																																																
Score: 1 Style: comparison	 <p>Explanation: Limited context is provided.</p>	Q: Analyze the image in a comprehensive and detailed manner. A: The image features a spacious living room with a clean and modern feel. There is a large, not red but rather brown, couch placed in the room, and a comfortable chair nearby, which is a wooden chair with fabric seat cover, situated away from the camera. A dining table is situated in the center of the room, surrounded by chairs, ...	Score: 1 Style: comparison																																																																	
Score: 0 Style: word/short phrase	<p>A. ①② B. ①④</p> <p>Explanation: No context-based learning is demonstrated.</p>	Q: 图中写了什么？请直接使用图中出现的文字回答，不用考虑上下文，只回答图中出现的文字。 A: A. ①② B. ①④	Score: 0 Style: word/short phrase																																																																	

Figure 19. Randomly selected samples from the LLaVA-OVSI data pool within each score group for the **object spatial understanding** capability, ranging from 5 to 0, as evaluated by GPT-4, along with corresponding score explanations and mmSSR predictions.

comparative	Image	QA Pairs	mmSSR																																																												
GPT4o Score: 5 Style: word/short-phrase, yes/no, comparison	 <p>Explanation: Strong need for comparing quantities across items.</p>	Q: Which item sold the most units? Answer the question with a single word. A: Victim Q: Which item sold the least units? A: Memory Q: How many units of the the most sold item were sold? A: 9 Q: How many units of the the least sold item were sold? A: 4 ...	Score: 4 Style: word/short-phrase, yes/no, comparison																																																												
Score: 4 Style: detailed description, comparison	 <p>Explanation: The comparison between messy and tidy states is clear.</p>	Q: Describe this image in detail with GPT-T-COCO format. A: The image presents a before-and-after comparison of a room undergoing a transformation from a messy state to a clean and tidy one. In the 'before' part of the image, the room is quite cluttered. There are books scattered about, a disorganized desk with a laptop on it, and a chair pushed askew. A suitcase is also visible, contributing to the sense of disarray. The 'after' part of the image showcases the same room, but with a considerable difference. It's noticeably tidier, with the books neatly stacked, the chair properly adjusted, and the laptop closed. The suitcase appears to be packed away, and the overall space looks much more organized...	Score: 4 Style: detailed description, comparison																																																												
Score: 3 Style: yes/no, word/short-phrase	<table border="1" data-bbox="394 940 646 1136"> <thead> <tr> <th colspan="5">Medal table</th> </tr> <tr> <th>Nation</th> <th>Gold</th> <th>Silver</th> <th>Bronze</th> <th>Total</th> </tr> </thead> <tbody> <tr> <td>Cyprus</td> <td>32</td> <td>30</td> <td>20</td> <td>82</td> </tr> <tr> <td>Luxembourg</td> <td>30</td> <td>15</td> <td>27</td> <td>72</td> </tr> <tr> <td>Iceland</td> <td>20</td> <td>23</td> <td>25</td> <td>68</td> </tr> <tr> <td>Malta</td> <td>8</td> <td>12</td> <td>9</td> <td>29</td> </tr> <tr> <td>Liechtenstein</td> <td>6</td> <td>10</td> <td>11</td> <td>27</td> </tr> <tr> <td>Monaco</td> <td>6</td> <td>9</td> <td>14</td> <td>29</td> </tr> <tr> <td>Montenegro</td> <td>4</td> <td>2</td> <td>2</td> <td>8</td> </tr> <tr> <td>Andorra</td> <td>3</td> <td>7</td> <td>5</td> <td>15</td> </tr> <tr> <td>San Marino</td> <td>3</td> <td>4</td> <td>11</td> <td>18</td> </tr> <tr> <td>Total</td> <td>112</td> <td>112</td> <td>124</td> <td>348</td> </tr> </tbody> </table> <p>Explanation: Involves comparing medal counts.</p>	Medal table					Nation	Gold	Silver	Bronze	Total	Cyprus	32	30	20	82	Luxembourg	30	15	27	72	Iceland	20	23	25	68	Malta	8	12	9	29	Liechtenstein	6	10	11	27	Monaco	6	9	14	29	Montenegro	4	2	2	8	Andorra	3	7	5	15	San Marino	3	4	11	18	Total	112	112	124	348	Q: cyprus win the most gold medal with 32, Yes or No? Answer the question using a single word or phrase. A: Yes	Score: 3 Style: yes/no, word/short-phrase
Medal table																																																															
Nation	Gold	Silver	Bronze	Total																																																											
Cyprus	32	30	20	82																																																											
Luxembourg	30	15	27	72																																																											
Iceland	20	23	25	68																																																											
Malta	8	12	9	29																																																											
Liechtenstein	6	10	11	27																																																											
Monaco	6	9	14	29																																																											
Montenegro	4	2	2	8																																																											
Andorra	3	7	5	15																																																											
San Marino	3	4	11	18																																																											
Total	112	112	124	348																																																											
Score: 2 Style: detailed description, specified style	 <p>Explanation: Some comparison is implied between the sandwiches.</p>	Q: Describe this image in detail with GPT-T-COCO format. A: The image depicts a restaurant scene where a large, appetizing sandwich is the center of attention. The sandwich, resting on a large plate, is piled high with rare roast beef, suggesting a corned beef sandwich. It's an open sandwich, with the slices of bread and layers of meat clearly visible... A second sandwich can be glimpsed further on the dining ...	Score: 1 Style: detailed description, specified style																																																												
Score: 1 Style: short description	 <p>Explanation: No comparison is required or possible.</p>	Q: Provide a one-sentence caption for the provided image. A: A dining room bathed in red light with a floral arrangement.	Score: 1 Style: short description																																																												
Score: 0 Style: word/short-phrase	 <p>Explanation: No comparison is required.</p>	Q: Transcribe visible text from this photograph. A: rendered in the Greek Revival style.	Score: 0 Style: word/short-phrase																																																												

Figure 20. Randomly selected samples from the LLaVA-OVSI data pool within each score group for the **attribute identification** capability, ranging from 5 to 0, as evaluated by GPT-4, along with corresponding score explanations and mmSSR predictions.



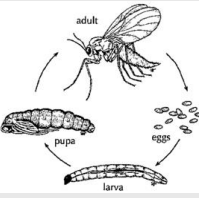

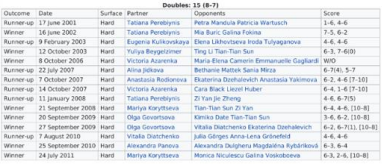
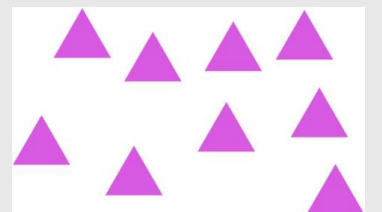
activity	Image	QA Pairs	mmSSR
GPT4o		<p>Q: Can you describe the main features of this image for me?</p> <p>A: In the heart of a bustling skatepark, a daring skateboarder is captured in mid-air, executing a thrilling trick on a wooden ramp. The skateboarder, dressed in a white shirt and beige pants, skillfully flips his skateboard beneath his feet, demonstrating his mastery and control. The ramp, the epicenter of the action, is situated in the middle of the frame. The atmosphere is vibrant and energetic. Several onlookers, some of whom are fellow skateboarders, ...</p>	<p>Score: 5</p> <p>Style: detailed description</p>
		<p>Q: Describe this image in detail with GPT-T-COCO format.</p> <p>A: The image captures a bustling city plaza filled with a diverse crowd of people. The crowd appears to be gathered for a demonstration, as suggested by the presence of signs and flags. The atmosphere is active and lively, with people standing, socializing, and moving around. Two people in the crowd are holding umbrellas, one of which is white. One person stands out as they are holding the umbrella in front of their face, creating an interesting visual effect. The other umbrella is positioned to the side of the image ...</p>	<p>Score: 4</p> <p>Style: detailed description, specified style</p>
		<p>Q: During which stage in its life cycle is the mosquito able to lay eggs? Choices: A. Adult B. pupa C. eggs D. larva Answer with the option's letter from the given choices directly.</p> <p>A: A</p> <p>Q: Which stage transforms into adult mosquito? Choices: A. Adult B. Larva C. Pupa D. Eggs Answer with the option's letter from the given choices directly.</p> <p>A: C</p>	<p>Score: 2</p> <p>Style: multi-choice</p>
		<p>Q: Why is the white lines on the glass? Answer the question using a single word or phrase.</p> <p>A: visibility. Rationale: The white lines are to increase visibility on the translucent glass preventing people or birds from colliding into it.</p>	<p>Score: 2</p> <p>Style: word/short phrase</p>
		<p>Q: zhang jie zheng be the opponent on 11 january , 2008, Yes or No? Answer the question using a single word or phrase.</p> <p>A: Yes</p>	<p>Score: 0</p> <p>Style: yes/no, word/short phrase</p>
		<p>Hint: Please answer the question and provide the correct option letter, e.g., A, B, C, D, at the end.</p> <p>Q: How many triangles are there? Choices: (A) 9 (B) 2 (C) 10 (D) 3 (E) 4</p> <p>A: The answer is A</p>	<p>Score: 0</p> <p>Style: multi-choice</p>

Figure 21. Randomly selected samples from the LLaVA-OVSI data pool within each score group for the logical deduction capability, ranging from 5 to 0, as evaluated by GPT-4, along with corresponding score explanations and mmSSR predictions.

causal	Image	QA Pairs	mmSSR
GPT4o		<p>Q: What would happen if all the lions died? Less deer Fewer owls More deer Caterpillars would be extinct Answer with the given options directly.</p> <p>A: More deer</p>	<p>Score: 5</p> <p>Style: word/sh ort-phrase</p>
	<p>Explanation: Strong causal reasoning is required to understand the impact of lions dying.</p>		
		<p>Q: Based on the vegetation and the snow conditions observed, what can be inferred about the likely elevation and climate conditions of this mountainous region?</p> <p>A: The presence of coniferous trees, which are typically found in subalpine and alpine zones, along with the extensive snow cover suggests that this region is at a high elevation, likely above the tree line where conditions are too harsh for most trees to survive. The snow appears to be fresh, indicating recent snowfall and possibly a cold ...</p>	<p>Score: 4</p> <p>Style: detailed description</p>
	<p>Explanation: Good causal reasoning about climate and elevation.</p>		
		<p>Q: Based on the image, what can be inferred about the nature of the troubleshooting process outlined in the slide, and how might it relate to the tasks performed by the Eastern Tennis Association?</p> <p>A: The troubleshooting process seems to be related to a scoring or record-keeping system, possibly for tennis matches, as the Eastern Tennis Association is involved with tennis. The first bullet point suggests a sequence that starts with "1" after the first server...</p>	<p>Score: 3</p> <p>Style: detailed description</p>
	<p>Explanation: Understanding cause-effect in the troubleshooting process.</p>		
		<p>Q: According to the question shown in the image, please first conduct reasoning, and then answer the question and provide the final value, e.g., The answer is xxx Question: Based on the image, what type of sequence is represented in the table?</p> <p>A: Review the differences between consecutive terms presented in the image to determine the type of sequence. Given the constant differences, the sequence is an arithmetic sequence. So the answer is arithmetic sequence. The answer is arithmetic sequence.</p>	<p>Score: 2</p> <p>Style: word/sh ort-phrase, chain-of-thought</p>
	<p>Explanation: Some relevance in understanding the cause of the sequence pattern.</p>		
		<p>Q: Tell me about the visual elements in this screen capture.</p> <p>A: Setup page of a hearing aid app.</p>	<p>Score: 1</p> <p>Style: short description</p>
	<p>Explanation: Minimal cause-effect information is present.</p>		
		<p>Q: What is the heading of the document? Answer the question using a single word or phrase.</p> <p>A: Executive Summary</p>	<p>Score: 0</p> <p>Style: word/sh ort-phrase</p>
	<p>Explanation: No causal reasoning is involved.</p>		

Figure 22. Randomly selected samples from the LLaVA-OVSI data pool within each score group for the **scene understanding** capability, ranging from 5 to 0, as evaluated by GPT-4, along with corresponding score explanations and mmSSR predictions.



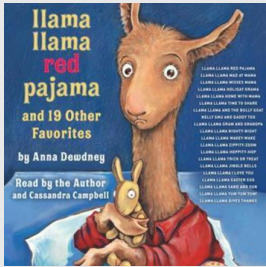

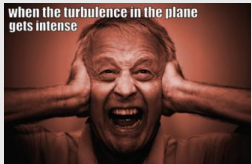

humanities	Image	QA Pairs	mmSSR
GPT4o		<p>Q: What is the role of the solitary figure with the pole in the dynamics of this scene?</p> <p>A: Based on the image and the title, the solitary figure with the pole is most likely Charon, the ferryman of Hades, who in Greek and Roman mythology, transports the souls of the newly deceased across the rivers Styx and Acheron that divided the world of the living from the world of the dead. His authoritative stance and detachment from the chaos suggest he is overseeing the embarkation of the souls to their final destination in the afterlife, indifferent to their pleas and suffering.</p>	<p>Score: 5</p> <p>Style: detailed description</p>
Score: 4		<p>Q: Can you describe the visual appearance of this image?</p> <p>A: Early 16th-century engraving of Toulouse</p>	<p>Score: 4</p> <p>Style: short description</p>
Score: 3		<p>Q: What is the title of the book mentioned in the image?</p> <p>A: The title of the book is "Llama Llama Red Pajama and 19 Other Favorites" by Anna Dewdney.</p> <p>Q: Who are the narrators of the book?</p> <p>A: The book is read by the author, Anna Dewdney, and Cassandra Campbell.</p> <p>Q: Can you list some stories or titles mentioned in the image?</p> <p>A: Some of the titles mentioned are: Llama Llama Red Pajama, Llama Llama Mad at Mama, Llama Llama Misses Mama, Llama Llama Holiday Drama, ...</p>	<p>Score: 3</p> <p>Style: word/short phrase, short description</p>
Score: 2		<p>Q: Considering the consistent background and the title indicating a cast interview, what can be inferred about the nature of the event where these photos were taken, and how do the individuals' attire and expressions contribute to the setting's informality or formality?</p> <p>A: The nature of the event can be inferred to be a promotional interview for the television show or movie "SERVANT." The consistency in the background across all six photos suggests they were taken at the same venue, likely set up for media interviews...</p>	<p>Score: 2</p> <p>Style: detailed description</p>
Score: 1		<p>Q: Can this meme be considered disrespectful? Answer the question using a single word or phrase.</p> <p>A: No.</p>	<p>Score: 1</p> <p>Style: yes/no, word/short phrase</p>
Score: 0		<p>Q: What's happening in the scene?</p> <p>A: In the image, a man clad in a vibrant red and black motorcycle suit stands next to a matching red and black motorcycle, prominently displayed in the center of the image. The motorcycle, leaning on its side stand, is parked in front of a red garage door adorned with multiple windows. The man, holding a helmet in his left hand, appears to be inspecting the motorcycle with a keen eye, standing very close to the camera...</p>	<p>Score: 0</p> <p>Style: detailed description</p>

Figure 23. Randomly selected samples from the LLaVA-OVSI data pool within each score group for the **fine-grained recognition** capability, ranging from 5 to 0, as evaluated by GPT-4, along with corresponding score explanations and mmSSR predictions.

STEM	Image	QA Pairs	mmSSR
GPT4o		<p>Q: According to the question shown in the image, please first perform reasoning, then finally select the right answer from the choices, e.g., Answer: xxx. Question: How would you calculate the perimeter of GF? Choices: A: 54.5 B: 46.5 C: 52.0 D: 41.03</p> <p>A: Since AB is 11.0 and ABCD is a rectangle, the opposite sides are the same length. Therefore, DC is also 11.0. DC equals 11.0. As DCEF is a square, all its sides are of equal length. Thus, DF = DC = 11.0. DF equals 11.0. As DFGH is a square, all its sides are of equal length. Thus, GF = DF = 11.0. With GF = 11.0 and angle I being 40°, ...</p>	<p>Score: 5</p> <p>Style: multi-choice, chain-of-thought</p>
		<p>Q: If the arc length of the ABC sector is 23.13 and the circumference of the lime semi-circle is 25.7, compute the degree of the CBA angle. Assume $\pi=3.14$. Round computations to 2 decimal places.</p> <p>A: The circumference of the lime semi-circle is 25.7 so the BC diameter can be computed as $\frac{25.7}{1 + \frac{3.14}{2}} = \frac{25.7}{2.57} = 10$. The BC radius of the ABC sector is 10 and the arc length is 23.13. So the CBA angle can be computed as $\frac{\text{ArcLength}}{2 \pi r} * 360 = \frac{23.13}{2 \pi * 10} * 360 = \dots$</p>	<p>Score: 5</p> <p>Style: detailed description</p>
		<p>Q: Are these items generally considered rose-like in their odor? Answer the question using a single word or phrase.</p> <p>A: No</p> <p>Q: What vitamin is the vegetable particular high in?</p> <p>A: Vitamin c</p> <p>Q: What color is the food?</p> <p>A: Green</p>	<p>Score: 2</p> <p>Style: yes/no, word/sh orth-phrase</p>
		<p>Q: Can you break down the data visualization and explain its message?</p> <p>A: The battle for independent voters remains tight. The current survey finds that 45% of independents back Romney and 43% Obama, which is virtually unchanged from earlier in July. Over the course of the year, independent support has wavered, with neither candidate holding a consistent advantage.</p>	<p>Score: 2</p> <p>Style: detailed description</p>
		<p>Q: What precautions should the man take while working in the rain? Answer the question with GPT-T-COCO format.</p> <p>A: While working in the rain, the man should take several precautions to ensure his safety and protect the items he handles. These precautions include wearing appropriate rain gear such as waterproof clothing, a raincoat, and footwear with slip-resistant soles to avoid potential slips and falls caused by wet surfaces. Additionally, he should exercise extra ...</p>	<p>Score: 1</p> <p>Style: detailed description</p>
		<p>Q: Is the bus moving? Answer the question using a single word or phrase.</p> <p>A: Yes</p> <p>Q: Is this a movie studio backlot?</p> <p>A: No</p> <p>Q: What is the primary color of the bus?</p> <p>A: Yellow</p> <p>Q: Is there any place of worship in the photo?</p> <p>A: No</p>	<p>Score: 0</p> <p>Style: yes/no, word/sh orth-phrase</p>

Figure 24. Randomly selected samples from the LLaVA-OVSI data pool within each score group for the **language generation** capability, ranging from 5 to 0, as evaluated by GPT-4, along with corresponding score explanations and mmSSR predictions.

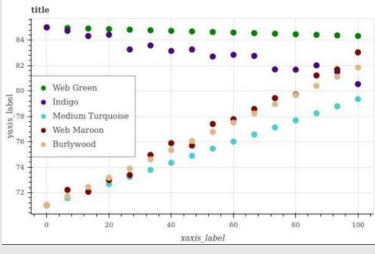
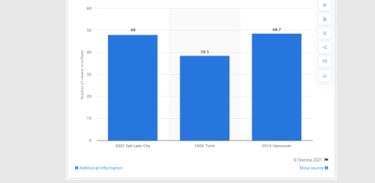
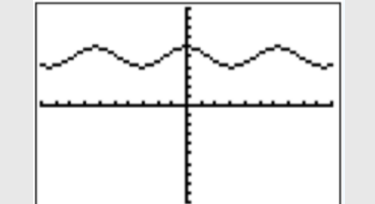



data	Image	QA Pairs	mmSSR
<p>GPT4o</p> <p>Score: 5</p> <p>Style: detailed description</p>	 <p>Explanation: Strong understanding of data representation in scatter plots.</p>	<p>Q: Write a detailed and comprehensive description of the image.</p> <p>A: The image is a scatter plot with five distinct categories represented by different colored markers. Each category is plotted against clearly defined x and y axes. ### Graph Elements: - Title: The plot has a placeholder for the title labeled "title". - X-axis Label: The x-axis is labeled "xaxis label". - Y-axis Label: The y-axis is labeled "yaxis label". ### Data Points: - Web Green: Represented by green circle markers. These points are clustered at the top of the plot around y values of approximately 82 to 86...</p>	<p>Score: 5</p> <p>Style: detailed description</p>
<p>Score: 4</p> <p>Style: word/short phrase</p>	 <p>Explanation: Significant as it involves interpreting a chart to extract information.</p>	<p>Q: What was the average minute rating of Olympic Winter Games broadcasts in Salt Lake City in 2002? Answer the question using a single word or phrase.</p> <p>A: 48.</p>	<p>Score: 3</p> <p>Style: word/short phrase</p>
<p>Score: 3</p> <p>Style: multi-choice, chain-of-thought</p>	 <p>Explanation: Involves knowledge of vitamins in vegetables.</p>	<p>Q: According to the question shown in the image, please first perform reasoning, then finally select the right answer from the choices, e.g., Answer: xxx.</p> <p>Question: Based on the image, what is the minimum value of the cosine function? Choices: A. -1 B. 0 C. 4 D. 5</p> <p>A: The minimum value of the cosine function can be identified as the lowest point of its cycle. With an amplitude of 1 and a vertical shift of 5, the minimum value is $5 - 1 = 4$. So the answer is C Answer: C</p>	<p>Score: 3</p> <p>Style: multi-choice, chain-of-thought</p>
<p>Score: 2</p> <p>Style: short description</p>	 <p>Explanation: The image includes structured text, useful for data understanding.</p>	<p>Q: Provide a one-sentence caption for the provided image.</p> <p>A: A translated page that is titled Attacking Ramsus' vessel!</p>	<p>Score: 2</p> <p>Style: short description</p>
<p>Score: 1</p> <p>Style: coordinate, short description</p>	 <p>Explanation: Basic data understanding in terms of object identification.</p>	<p>Q: Provide a short description for the given region.</p> <p>[0.658,0.832,0.816,0.925]</p> <p>A: A blue and white truck.</p> <p>Q: [0.738,0.853,0.964,0.963]</p> <p>A: A silver car.</p> <p>Q: [0.280,0.840,0.456,0.939]</p> <p>A: A white house.</p> <p>Q: [0.138,0.915,0.172,0.973]</p> <p>...</p>	<p>Score: 0</p> <p>Style: coordinate, short description</p>
<p>Score: 0</p> <p>Style: short description, word/short phrase</p>	 <p>Explanation: No data or charts to interpret.</p>	<p>Q: What color is the handle of the knife? Answer the question using a single word or phrase.</p> <p>A: Green</p> <p>Q: What is the man doing?</p> <p>A: Cutting apple</p> <p>Q: What type of apple is he holding?</p> <p>A: Red</p>	<p>Score: 0</p> <p>Style: short description, word/short phrase</p>

Figure 25. Randomly selected samples from the LLaVA-OVSI data pool within each score group for the **in-context learning** capability, ranging from 5 to 0, as evaluated by GPT-4, along with corresponding score explanations and mmSSR predictions.

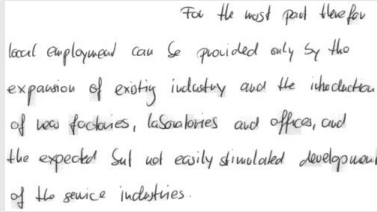

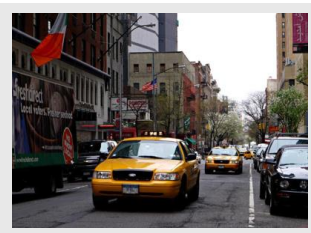
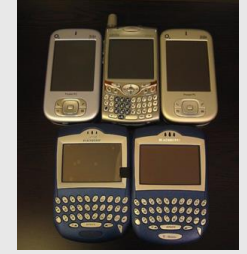

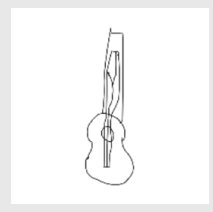
OCR	Image	QA Pairs	mmSSR
GPT4o			
Score: 5 Style: detailed description	<p>For the most part therefore local employment can be provided only by the expansion of existing industry and the introduction of new factories, laboratories and offices, and the expected but not easily stimulated development of the service industries.</p> <p>Explanation: The instance provides a clear example of handwritten text recognition, which is highly relevant for OCR capability.</p>	<p>Q: What is scribbled in this image? A: For the most part therefore local employment can be provided only by the expansion of existing industry and the introduction of new factories, laboratories and offices, and the expected but not easily stimulated development of the service industries.</p>	Score: 5 Style: detailed description
Score: 4 Style: detailed description	 <p>Explanation: The description includes details about the text on the card, aiding OCR capabilities.</p>	<p>Q: Describe this image in detail. A: The image displays a golden business card with intricate, laser-cut detailing around the edges. The card features a mix of English and Chinese text. In the upper portion, the Chinese characters are prominent, and below them, the English translation reads "Personal Tailor." The text is printed in red with a shimmering effect that contrasts with the metallic sheen of the gold card. The card's design is elegant and suggests a personalized service, ...</p>	Score: 4 Style: detailed description
Score: 3 Style: short description	 <p>Explanation: The image contains text on the truck, which can be recognized.</p>	<p>Q: Write a terse but informative summary of the picture. A: The yellow taxi drives next to a freshdirect truck.</p>	Score: 3 Style: short description
Score: 2 Style: short description	 <p>Explanation: Some text is visible on the devices but not the main focus.</p>	<p>Q: Provide a one-sentence caption for the provided image. A: Five different types of cellular phones next to each other on a table.</p>	Score: 2 Style: short description
Score: 1 Style: detailed description	 <p>Explanation: Minimal relevance as there is text in the image but not utilized.</p>	<p>Q: Considering the presence of multiple bottles in the scene, what issue does this environment illustrate, and how can it affect pedestrians? Answer the question with GPT-T-COCO format. A: The environment in the image shows an issue of littering, as multiple bottles are scattered across the scene near the road. This can negatively affect pedestrians in several ways, such as creating a dirty and unkempt surrounding, posing health risks, ...</p>	Score: 0 Style: detailed description
Score: 0 Style: multi-choice	 <p>Explanation: No text is present in the image.</p>	<p>Q: You will be given an image of a guitar. The image could be of different categories like painting, cartoon, photograph, or sketch. Identify the image category. Options: (a) Photograph (b) Cartoon (c) Art painting (d) Sketch A: (d) Sketch</p>	Score: 0 Style: multi-choice

Figure 26. Randomly selected samples from the LLaVA-OVSI data pool within each score group for the **optical character recognition** capability, ranging from 5 to 0, as evaluated by GPT-4, along with corresponding score explanations and mmSSR predictions.